Experimental Investigations of the Electronic Band Structure of Solids*

BENJAMIN LAX

Lincoln Laboratory, Massachusetts Institute of Technology, Lexington, Massachusetts

INTRODUCTION

THE tremendous interest in the band structure of solids in recent years has resulted from the simultaneous efforts of theoreticians, who have attempted to calculate the band structure from first principles, and the experimentalists, who have been carrying on extensive investigations of the electrical, magnetic, and optical properties of both single crystal and polycrystalline semiconductors and metals. Although the theoretical physicists have made momentous strides in determining the character and nature of the energy bands, they were often limited in correctly predicting the quantitative nature of these bands. Nevertheless, where results existed, their work formed a very useful guide for analyzing experimental results. The latter provided information which could be used in modifying and extending the theoretical calculations. Such mutual interplay of effort was beautifully displayed in the resolution of the complicated band structure of germanium and silicon and more recently indium antimonide and graphite.

The paper by F. Herman[1] has outlined the achievements of current theoretical methods in determining the band structure of some of the well-known semiconductors and metals and in discussing those features which have an important bearing on the electrical and optical properties. In this paper a class of experiments is discussed which have played significant roles in contributing to our present understanding of the band structure of many materials of current interest. In particular, experiments on the de Haas-van Alphen effect, cyclotron resonance, galvanomagnetic effect, and infrared absorption are discussed. The cyclotron resonance experiments include those at microwave and infrared frequencies. The infrared absorption experiments involve interband transitions and the more recent oscillatory magnetoabsorption effect in semiconductors.

Historically the galvanomagnetic measurements, such as that of the Hall effect and magnetoresistance, were the earliest, and were instrumental in shedding light on the nature of bands in metals. Even today, the galvanomagnetic techniques are still very useful for exploratory purposes. Among the more classic methods, the de Haas-van Alphen effect is perhaps the most powerful tool in that it provides quantitative and direct information on the curvature of bands at the Fermi surface in metals. The oscillatory Hall, thermomagnetic and magnetoresistance effects are essentially another form of the de Haas-van Alphen phenomenon, and do not provide additional information about the bands. The most powerful and direct method by far is the cyclotron resonance, where it is feasible. In germanium and silicon the extent of its success is not equaled by any of the other methods. In the infrared region this technique has been instrumental in exploring the variation of the band curvature beyond the minimum of the conduction band in indium antimonide and in bismuth possibly above the Fermi surface. The infrared absorption measurements have been used to determine the energy separation of the bottom of the conduction and top of the valence bands in semiconductors. More recently, refined measurements have been made to determine the detailed nature of the absorption edge and have provided information on the location of the band extrema in the Brillouin zone. Variation of the absorption edge with doping of such semiconductors as indium antimonide and indium arsenide also provides information on the curvature of the conduction and valence bands in these materials. Infrared absorption experiments in p-type material, involving interband transitions in the valence bands of germanium subsequent to the cyclotron resonance results, were effective in confirming the theoretical work. By far the most promising infrared tool is the newly discovered oscillatory magnetoabsorption effect. This has already provided information on higher bands in germanium on the conduction band spin orbit effect in indium antimonide and the conduction band in indium arsenide. The oscillatory magnetoabsorption has also suggested the nature of the transition processes near the absorption edge in these materials. The magnetoabsorption technique should be successful in investigating some of the band properties of many of the new semiconductors in which cyclotron resonance and galvanomagnetic experiments have not been possible.

CYCLOTRON RESONANCE

Microwave Experiments in Semiconductors

Although galvanomagnetic and magnetic susceptibility measurements in solids are older than cyclotron resonance experiments, the latter are simpler and more direct. Consequently it is logical to start with cyclotron resonance. The phenomenon has been quite familiar to the ionospheric physicists who were concerned with the

* The research reported in this document was supported jointly by the U. S. Army, Navy, and Air Force under contract with the Massachusetts Institute of Technology.

[1] F. Herman, Revs. Modern Phys. **30**, 102 (1958), preceding paper.

propagation of radio-frequency waves through the ionosphere in the presence of the earth's magnetic field.[2] The effect has also been observed in the laboratory at ultra-high frequencies (uhf)[3] and studied quantitatively at microwave frequencies by the MIT gas discharge group.[4] An electron moves in a helical path in the presence of a dc magnetic field **H** and rotates about the magnetic field with the cyclotron frequency

$$\omega_c = eH/m^*c. \tag{1}$$

When an rf electric field transverse to **H** interacts with the electron, then the electron, in addition to its rotational motion, also executes oscillatory motion simultaneously at a frequency ω corresponding to the frequency of the electric field. When this frequency is equal to the cyclotron frequency, i.e., $\omega=\omega_c$, the electron executes a spiral motion in the plane perpendicular to **H** after steady-state conditions are established. The steady increase in energy as the radius of the spiral increases cannot go on indefinitely because the electron eventually collides with an atom or molecule. In a solid, the mean free time, τ, is determined by lattice scattering due to thermal vibrations, or by collisions with impurity atoms or imperfections. If the electron traces out only a small fraction of a cycle, the effect of the magnetic field on the energy exchange between the electron and the rf electric field is negligible. However, if τ is sufficiently long to permit the electron to complete one or more rotations between collisions, then energy transfer between electron and electric field is enhanced. Absorption as a function of applied magnetic field for different values of the product of frequency and the scattering time is shown in Fig. 1. The absorption is proportional to $[1+(\omega-\omega_c)^2\tau^2]^{-1}+[1+(\omega+\omega_c)^2\tau^2]^{-1}$. When $\omega\tau\geq 1$, the absorption shows a resonance peak at $\omega=\omega_c$ for high $\omega\tau$. The frequency of the resonance peak can be used as a means of determining the effective mass of the electron, since the frequency ω and the magnetic field **H** can be measured, and m^* is unknown. The mass m^*

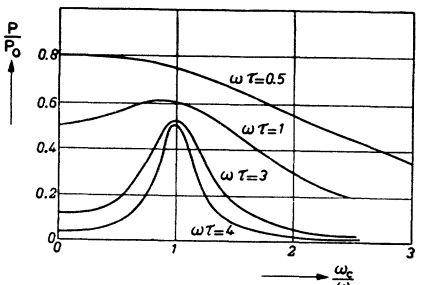

FIG. 1. Theoretical curves of cyclotron absorption as a function of magnetic field **H** in germanium. Magnetic field along the [100] axis, and rf electric field transverse to it. The power P_{100} is normalized by the power P_0 when $H=0$ and $\omega=0$. (After Lax, Zeiger, and Dexter.)

[2] E. V. Appleton, U.R.S.I. Reports, Washington (1927).
[3] J. S. Townsend and E. W. B. Gill, Phil. Mag. **26**, 290 (1938); A. E. Brown, Phil. Mag. **29**, 302 (1940).
[4] Lax, Allis, and Brown, J. Appl. Phys. **21**, 1297 (1950).

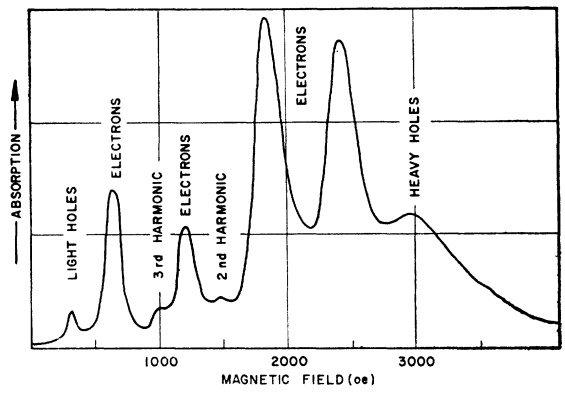

FIG. 2. Copy of cyclotron resonance trace in germanium near 4°K and 23 000 Mc/sec; external magnetic field was about 10° out of (110) plane and 30° from [100] direction. Orientation selected to show the eight resonances observed in germanium. (After Dexter, Zeiger, and Lax.)

is known as the effective mass and differs from the free mass because the charge carrier moves in the periodic field of the lattice. On solving the appropriate Schroedinger equation, taking this into account, the following energy-momentum relation is obtained for an isotropic carrier:

$$\epsilon = p^2/2m^*, \tag{2}$$

where $1/m^*=\partial^2\epsilon/\partial p^2$ is a measure of the curvature of the energy band associated with the motion of the electron. The effective mass is more generally a tensor represented by $1/m^*=\text{grad}_p\,\text{grad}_p\epsilon$.

The principal objective of the cyclotron resonance experiments is to investigate quantitatively the curvature of the bands by measuring the mass tensor of the electrons or holes associated with the appropriate surfaces in the Brillouin zone. The theory of cyclotron resonance as applied to solids was first discussed by Dorfman[5] and Dingle.[6] However, the first clear proposal for such an experiment was made by Shockley[7] who outlined the scheme for germanium. The first experiments were carried out at Berkeley.[8] Complete experiments which measured anisotropy parameters of the energy surfaces of electrons and holes in germanium were reported shortly thereafter by the Lincoln group.[9,10]

The experiments were carried out by placing oriented single crystals in a microwave cavity immersed in a helium bath. This reduced the dominant source of scattering in pure germanium, i.e., lattice vibrations. The carriers were frozen into impurity levels so that the crystal behaved essentially as an insulator. In the early

[5] J. Dorfman, Doklady Acad. Nauk. SSSR **81**, 765 (1951).
[6] R. B. Dingle, Ph.D. thesis, Cambridge University, 1951 (unpublished); *Proceedings of the International Conference on Very Low-Temperatures*, edited by R. Bowers (Oxford University Press, New York, 1951), p. 165; Proc. Roy. Soc. (London) **A212**, 38 (1952).
[7] W. Shockley, Phys. Rev. **90**, 491 (1953).
[8] Dresselhaus, Kip, and Kittel, Phys. Rev. **92**, 827 (1953).
[9] Lax, Zeiger, Dexter, and Rosenblum, Phys. Rev. **93**, 1418 (1954).
[10] Dexter, Lax, and Zeiger, Phys. Rev. **95**, 557 (1954).

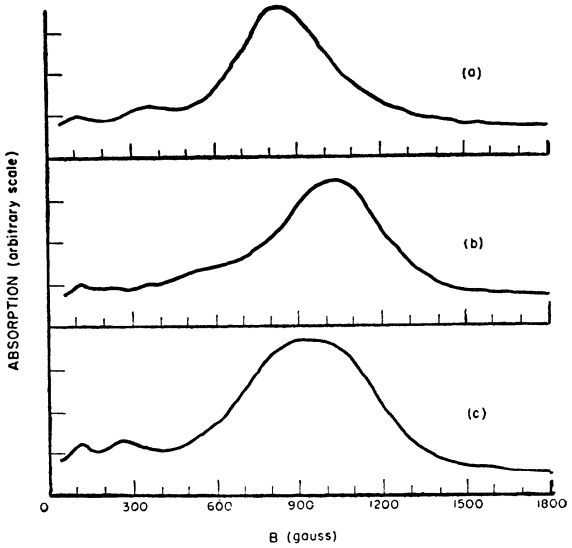

FIG. 3. Resonance absorption of holes in p-type Ge at 8900 Mc/sec, with infrared excitation. (a), (b), and (c) represent **B** along [001], [111], and [110] directions, respectively. Intermediate peak is weak resonance due to electrons. (After Lax, Zeiger, and Dexter.)

experiments on germanium,[9] carriers were re-excited into the conduction or valence band by impact ionization, which was induced by raising the microwave energy fed into the cavity to the suitable level. This scheme was utilized by the Lincoln group in identifying the holes or electrons which were selectively excited depending on whether the specimen was p type or n type, as determined by Hall measurements at liquid nitrogen temperatures. The Berkeley group used circularly polarized microwaves to distinguish between holes or electrons.[8,11] In later experiments light was used to ionize the frozen impurities.[11–14] This had the advantage of producing very sharp resonant lines. When only white light was used, the quanta of high energy excited both holes and electrons, as shown in Fig. 2. A properly selected infrared source permitted relatively selected excitation of either holes or electrons, again depending on the type of impurity concentration. Such a scheme was needed for observing the anisotropy of the heavy hole in germanium, as shown in Fig. 3. Impact ionization obscured the anisotropy of the holes in germanium. In silicon, impact ionization failed altogether. Here again optical excitation was necessary. Once the carriers were induced into the conduction or valence bands, the dc magnetic field surrounding the Dewar and the microwave cavity was automatically swept. Resonance was observed by taking an automatic trace of the microwave signal reflected from the cavity. Such a trace is shown in Fig. 2. Others were also obtained for a series of orientations with the magnetic field in the (110) plane of the crystal.

The anisotropy of the resonance peaks which are shown for electrons in Fig. 4 for silicon and in Fig. 5 for germanium can be analyzed as follows: The data suggest that the energy surfaces can be represented by families of ellipsoids which must be consistent with the cubic symmetry of the crystals. The simplest possible combinations may be three or six ellipsoids of revolution along the cube edges or [100] axes and four or eight ellipsoids of revolution along the cube diagonal or [111] axis. The three or four apply if the energy minima associated with the conduction band are located at the edges of the Brillouin zone and the six or eight are appropriate if the minima are inside the zone. For silicon, only a single resonance peak is obtained when the magnetic field is parallel to the [111] direction. This single resonance indicates that the ellipsoids are along the [100] direction since all such ellipsoids appear equivalent with respect to the cube diagonal. Similarly, for germanium the single resonance peak occurs with H along the [100] direction indicating that the ellipsoids must lie along the [111] or cube diagonals. With this in mind, the components of the mass tensor of each ellipsoidal surface can be derived from

$$\epsilon=\frac{p_x^2+p_y^2}{2m_t}+\frac{p_z^2}{2m_l}, \tag{3}$$

where m_l is the effective mass along the principal axis of the ellipsoid and m_t is the transverse mass. The effective mass m^* corresponding to the resonance peak and that of Eq. (1) is given by

$$m^*=m_t\left(\frac{m_l}{m_l\cos^2\theta+m_t\sin^2\theta}\right)^{\frac{1}{2}}, \tag{4}$$

where θ is the angle between the magnetic field and the principal axis of the ellipsoid. Two experimental values

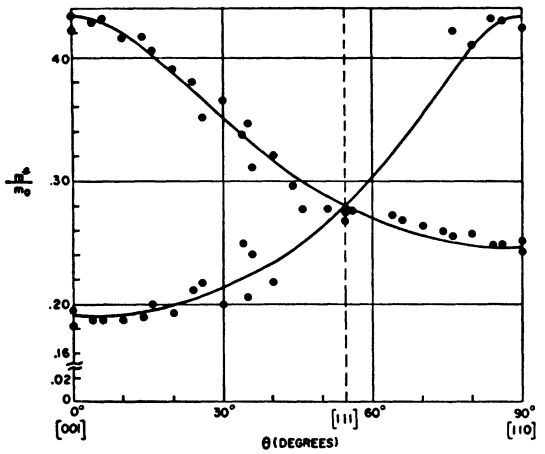

FIG. 4. Effective mass of electrons in silicon as a function of magnetic field orientation in the (1̄10) plane. (After Dexter, Lax, Kip, and Dresselhaus.)

[11] A. F. Kip, Physica **20**, 813 (1954).
[12] Lax, Zeiger, and Dexter, Physica **20**, 818 (1954).
[13] Dexter, Lax, Kip, and Dresselhaus, Phys. Rev. **96**, 222 (1954).
[14] R. N. Dexter and B. Lax, Phys. Rev. **96**, 223 (1954).

of m^* were selected from the measured values of H. Using the two corresponding values of θ for these masses, m_l and m_t were calculated from Eq. (4). The values obtained for electrons[15] are as follows:

Si: $m_l=(0.98\pm0.04)m_0$, $m_t=(0.19\pm0.01)m_0$,

Ge: $m_l=(1.64\pm0.03)m_0$, $m_t=(0.0819\pm0.0003)m_0$,

where m_0 is the mass of the free electron. Analogously the anisotropy data for hole resonance was obtained with the magnetic field again rotated in the (110) plane. The plot of the two effective masses of the holes as a function of the rotational angle is shown in Fig. 6 for silicon. A similar plot has also been obtained for germanium. The interpretation of the data can be made by using the theoretical expressions developed by Dresselhaus, Kip, and Kittel.[16,17] Their development was based on the existence of two kinds of holes which suggested two degenerate bands at the center of the zone. The threefold degeneracy has been removed by spin orbit splitting lowering the third band below that of the others. The results of the perturbation theory which uses group theory and takes into account the symmetry properties of the crystal give the following expressions for the energy momentum relations of the three bands

$$\epsilon_{1,2}=-\frac{1}{2m_0}\times[Ap^2\pm(B^2p^4+C^2(p_x^2p_y^2+p_x^2p_z^2+p_y^2p_z^2))^{\frac{1}{2}}], \quad (5)$$

$$\epsilon_3=-\Delta-(1/2m_0)Ap^2,$$

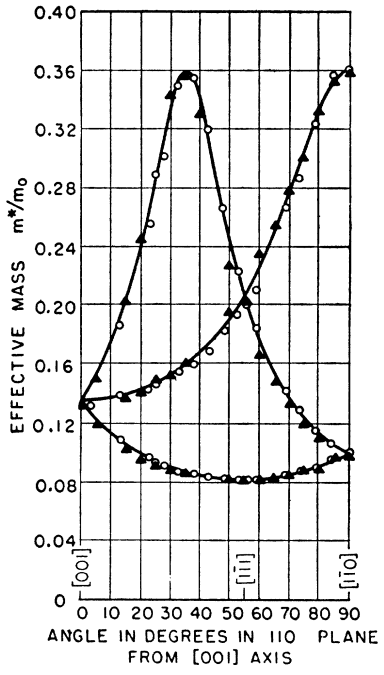

FIG. 5. Effective mass of electrons in germanium at 4°K for magnetic field directions in a (110) plane. Theoretical curves calculated from Eq. (4). (After Dresselhaus, Kip, and Kittel.)

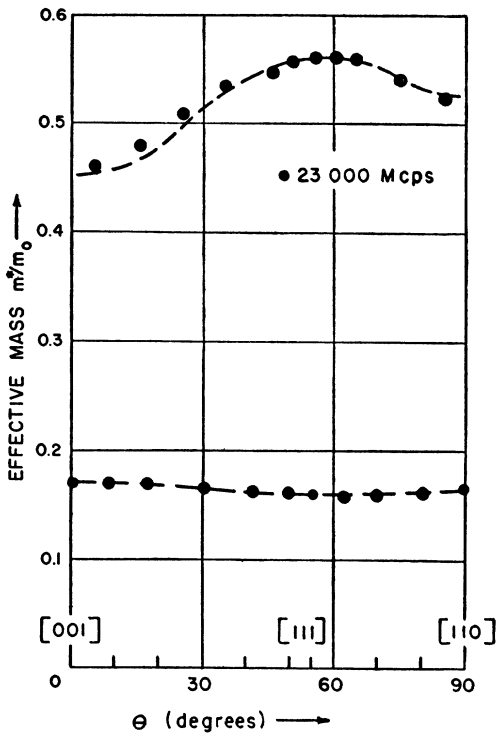

FIG. 6. Effective masses of holes in silicon; magnetic field in the (110) plane. Curves are theoretical and points experimental. (After R. N. Dexter, doctoral thesis, University of Wisconsin, 1955.)

where A, B, and C are constants which can be determined from the cyclotron resonance experiments, Δ is the spin orbit splitting energy and the plus sign refers to the surface of the light hole and the minus sign to that of the heavy hole. Shockley[18] suggested a method for evaluating the constants in which the effective mass for the warped surfaces represented by Eq. (5) is given by the integral of the form

$$m^*=\frac{1}{2\pi}\oint\frac{pd\phi}{\partial\epsilon/\partial p} \quad (6)$$

in which the energy surfaces of Eq. (5) have been transformed into cylindrical coordinates and have the following form when $p_H=0$

$$\epsilon=-\frac{p^2}{2m_0}[A\pm\{B^2+\tfrac{1}{4}C^2[1+g(\theta,\phi)]\}^{\frac{1}{2}}], \quad (7)$$

$$g(\theta,\phi)=(3\cos^2\theta-1)[(\cos^2\theta-3)\cos^4\phi+2\cos^2\phi],$$

where θ is the angle the magnetic field makes with the [100] axis in the (110) plane, and ϕ is the azimuthal angle in the plane perpendicular to the magnetic field with p_H, the component parallel to the magnetic field equal to zero. This gives an approximate expression[17]

[15] Dexter, Zeiger, and Lax, Phys. Rev. **104**, 637 (1956).
[16] Dresselhaus, Kip, and Kittel, Phys. Rev. **95**, 568 (1954); C. Kittel, Physica **20**, 829 (1954).
[17] Dresselhaus, Kip, and Kittel, Phys. Rev. **98**, 368 (1955).
[18] W. Shockley, Phys. Rev. **79**, 191 (1950).

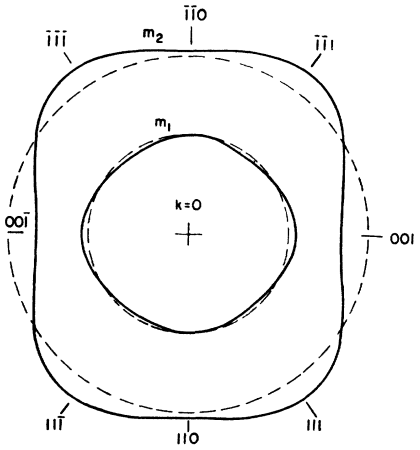

FIG. 7. Cross section of the constant energy contour in momentum space $\epsilon(\mathbf{k})$ *vs* $\mathbf{k}$, in the (110) plane for the valence band in silicon. The wave vector $\mathbf{k}$ is proportional to the momentum and m_1 and m_2 designate masses of the light and heavy holes, respectively. (After Dexter, Zeiger, and Lax.)

for the effective mass:

$$\frac{m^*}{m_0} \approx \frac{1}{A \pm [B^2+(C/2)^2]^{\frac{1}{2}}} \times \left\{ 1 \pm \frac{C^2(1-3\cos^2\theta)^2}{64[B^2+(C/2)^2]^{\frac{1}{2}}\{A \pm [B^2+(C/2)^2]^{\frac{1}{2}}\}} + \cdots \right\}. \tag{8}$$

Using this equation for three suitable experimental values from Fig. 6 for silicon (or from similar data for germanium), one evaluates A, B, and C. A more exact treatment using the Boltzmann transport theory, which takes into account the different values of p_H and also the scattering time which influences the line shape, has been carried out by Zeiger, Lax, and Dexter.[19] Using this theory the results[15] are:

	A	B	C
Ge:	13.1±0.4,	8.3±0.6,	12.5±0.5,
Si:	4.0±0.1,	1.1±0.4,	4.1±0.4.

These calculations indicate that the energy surfaces of the valence band in germanium and silicon consist of two concentric warped spheres, which for the heavy hole protrude in the [111] directions. For the light holes the surfaces are depressed along the [111] and protrude along the [100] directions. Cross sections of such surfaces are shown in Fig. 7 for silicon for a slice in a (110) plane, with $p_H=0$.

From these results and the theoretical work,[20] one can draw energy surface diagrams (Fig. 8) for germanium and silicon, which are relatively well developed in comparison with other materials. The perturbation theory for germanium also predicted the curvature of a higher conduction band Γ_2^- at the center of the zone with a mass $m^* \approx 0.034 m_0$.[17] The location of this band, the split-off valence band, and the relative position of the minima have been determined from infrared and other experiments discussed later. It turns out that the [111] conduction band minima for germanium are at the edge of the zone, and [100] conduction band minima for silicon are between the center and the edge of the Brillouin zone.

Luttinger and Kohn[21] carried out a quantum mechanical treatment of cyclotron resonance for holes, which is applicable to germanium and silicon. Their work indicated that cyclotron resonance consists of a transition between neighboring quantized magnetic levels. For low quantum numbers, the spacing between these levels is unequal, and they predicted that under the appropriate experimental conditions, fine structure would be superimposed on the resonance lines of holes, and the resonant frequencies would change. Fletcher, Yager, and Merritt[22] carried out these experiments using very pure samples of germanium at 4.2 and 1.3°K and obtained the narrowest resonance lines observed to date

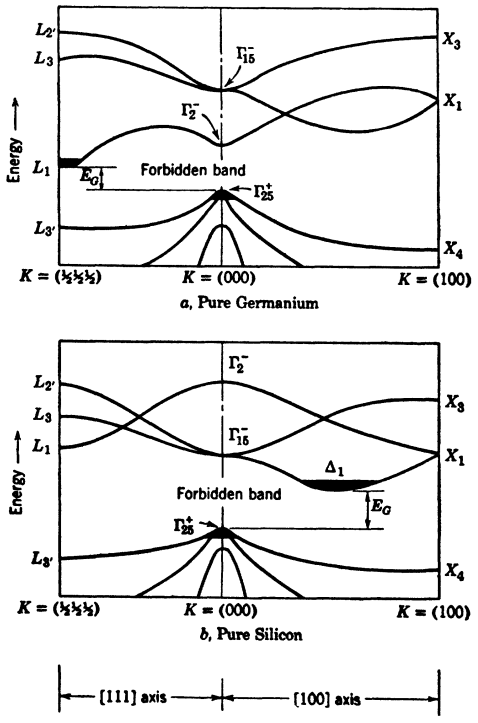

FIG. 8. Schematic diagrams of the energy band contours in germanium and silicon along the [111] and [100] axes in the Brillouin zone. The darkened portions designate the maxima and the minima of the valence and conduction bands. The split-off valence band below the degenerate bands is produced by spin-orbit interaction. [After F. Herman, Phys. Rev. **95** 847 (1954).]

[19] Zeiger, Lax, and Dexter, Phys. Rev. **105**, 495 (1957).
[20] F. Herman and J. Callaway, Phys. Rev. **89**, 518 (1953); F. Herman, Phys. Rev. **93**, 1214 (1954); F. Herman, Phys. Rev. **95**, 847 (1954); F. Herman, Physica **20**, 801 (1954); Proc. Inst. Radio Engrs. **43**, 1703 (1955).
[21] J. M. Luttinger and W. Kohn, Phys. Rev. **97**, 869 (1955).
[22] Fletcher, Yager, and Merritt, Phys. Rev. **100**, 747 (1955).

at microwave frequencies. They observed fine structure and confirmed qualitatively the existence of these quantum effects. No quantitative correlation between theory and experiment was given.

In addition to quantum effects, other phenomena associated with the warping of the energy surface of the heavy holes was observed. Kip[11] reported the presence of extra lines in an early paper on cyclotron resonance. These lines were also observed by Dexter, Zeiger, and Lax[15] in both silicon and germanium and clearly shown to be harmonics associated with the nonlinear motion of the heavy hole in the presence of the magnetic field. These harmonics which are shown in Fig. 2 were analyzed theoretically by Zeiger, Lax, and Dexter[19] and correlated with experiments.

Cyclotron resonance experiments have been carried out on germanium-silicon alloys,[23] but the results were not conclusive since the resolution was rather poor due to the large scattering. If the curvature of the bands were different from that of germanium or silicon with small alloying content, the accuracy of the experiments failed to show this adequately. Other semiconductors were also tried with little success. Only indium antimonide provided even limited success. The first results of Dexter and Lax[24] with $\omega\tau\approx\frac{1}{3}$ gave an extrapolated value for the electron mass, $m^*\approx 0.02m_0$. At Berkeley, improved resolution[25] for p-type material gave an electron mass $m_e^*\approx 0.013m_0$ with no anisotropy and a hole mass $m_h^*\approx 0.18m_0$ with unresolvable but definite anisotropy. The experimental resonance spectrum for indium antimonide gave a well-resolved peak for electrons and a broad resonance for the holes.

Microwave Cyclotron Resonance in Metals

Although cyclotron resonance was first proposed for metals, experiments on metals followed those in semiconductors. Early unpublished experimental results by the Berkeley group on graphite and the Lincoln group on bismuth did not show resonance. The former group proved theoretically that one obtains nonresonant absorption in metals at microwave frequencies.[26] This was soon followed by reports of cyclotron absorption in bismuth by Galt and co-workers[27] and also Dexter and Lax.[28] The latter clearly demonstrated that although the absorption is nonresonant, there is an inflection point in the curve as a function of magnetic field near resonance, given by

$$\omega_c=\omega+K/\tau, \tag{9}$$

where K is a constant near unity. Using this approach, the Lincoln group[29] and M. Tinkham[30] showed that the

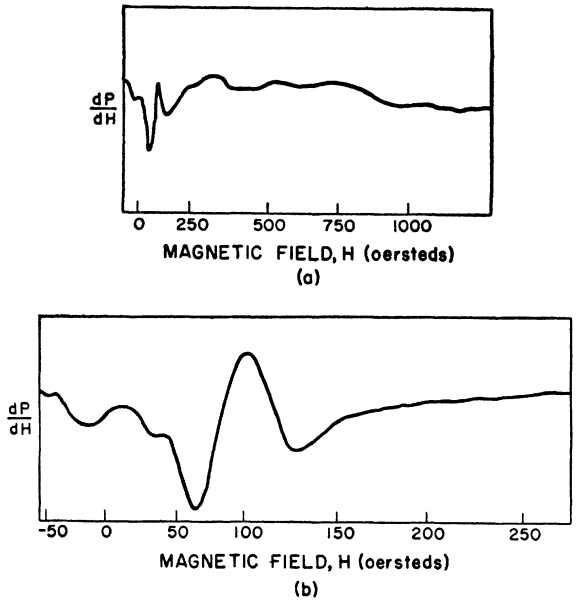

FIG. 9. The derivative trace of cyclotron resonance absorption in bismuth with the magnetic field parallel to the surface of the sample in the trigonal plane. (b) is a magnification of the low-field portion of (a). (After Foner, Zeiger, Powell, Walsh, and Lax.)

experimental results were roughly consistent with those of the de Haas-van Alphen results, discussed later. More recent experiments[31] confirm the order-of-magnitude agreement between the de Haas-van Alphen masses and the cyclotron resonance masses. However, anisotropy of the cyclotron resonance spectra does not agree with simple classical theory,[29] using Shoenberg's data for electron masses in Bi. Figure 9(a) shows the experimental results obtained by the Lincoln group for the derivative trace of power absorption as a function of dc magnetic field, with the dc field parallel to the $[11\bar{2}0]$ direction in the trigonal plane of a Bi sample. The curves show three peaks at $\sim$100, 200, and 300 oersteds. These give mass values of $\sim 0.01m_0$, $0.015m_0$, and $0.02m_0$, respectively, where the latter two have been corrected for the shift of the inflection point using Eq. (9). The de Haas-van Alphen masses for electrons with H along this crystallographic direction are $0.008m_0$ and $0.016m_0$. The peaks at 200 and 300 oersteds are poorly resolved, but appear to be anisotropic, and are perhaps associated with the de Haas-van Alphen electron masses. The well-resolved peak at 100 oersteds appears to be isotropic in the trigonal plane. Figure 9(a) also shows some broad unresolved structure at higher fields. Figure 9(b) shows a more detailed trace of derivative absorption at low dc fields. In addition to the peak at $\sim$100 oersteds, two small peaks appear at lower fields which also appear to be isotropic in the trigonal plane. Two possible explanations of the origin of these three peaks suggest themselves. (1) Existence of minority

[23] Dresselhaus, Kip, and Kittel, Phys. Rev. **100**, 1218 (1955).
[24] R. N. Dexter and B. Lax, Phys. Rev. **99**, 635 (1955) (A).
[25] Dresselhaus, Kip, Kittel, and Wagoner, Phys. Rev. **98**, 556 (1955).
[26] Dresselhaus, Kip, and Kittel, Phys. Rev. **100**, 618 (1955).
[27] Galt, Yager, Merritt, Cetlin, and Dail, Phys. Rev. **100**, 748 (1955); P. W. Anderson, Phys. Rev. **100**, 749 (1955).
[28] R. N. Dexter and B. Lax, Phys. Rev. **100**, 1216 (1955).
[29] Lax, Button, Zeiger, and Roth, Phys. Rev. **102**, 715 (1956).
[30] M. Tinkham, Phys. Rev. **101**, 902 (1956).
[31] Foner, Zeiger, Powell, Walsh, and Lax, Bull. Am. Phys. Soc. Ser. II, **1**, 117 (1956).

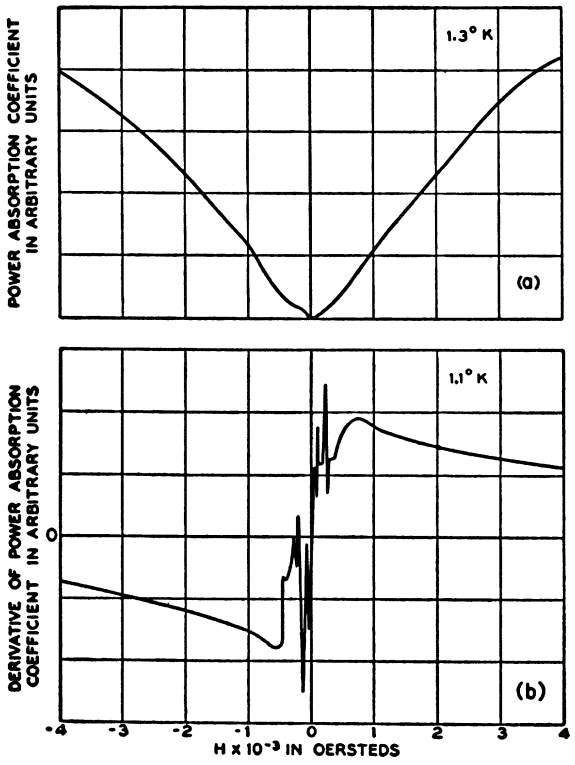

FIG. 10. (a) Plot of power absorption coefficient *vs* dc magnetic field for circularly polarized radiation at 24 000 Mc/sec at normal incidence on the (00.1) plane of graphite at 1.3°K. The magnetic field is normal to the (00.1) plane. The vertical scale is only approximately linear. Zero absorption is somewhere below the axis of abscissas. Cyclotron resonance for electrons will occur on the negative side of $H=0$, that for holes on the positive side. (b) Plot of derivative of curve shown in (a) as observed experimentally in an independent experiment done at 1.1°K with a field modulation method. (After Galt, Yager, and Dail.)

carriers not detected by the de Haas-van Alphen effect. (2) The peak at ~100 oe is a minority carrier peak, and two lower field peaks are subharmonics associated with the Azbel and Kaner effect, discussed later.

Experiments on bismuth and the related theoretical work demonstrate that for the study of microwave cyclotron resonance in metals, it is desirable to use circular polarization, with the dc magnetic field perpendicular to the surface of the sample. This permits a more direct interpretation of the derivative peaks and also separates the resonance of the holes and electrons. If the magnetic field is parallel to the sample surface, the resonance peaks for both holes and electrons in pure samples appear together. Furthermore, interpretation is more difficult, even in doped materials where one type of carrier dominates, because the peaks for multiple energy surfaces in this configuration in the classical limit do not correspond to the true cyclotron resonances.[29] A beautiful demonstration of the circular polarization method was given by Galt, Yager, and Dail in their experiment on graphite.[32] Their curves for the absorption and the corresponding derivative traces are shown in Fig. 10. The shape of the absorption curve clearly indicates that the graphite crystal was fairly pure and that the hole and electron concentrations must be about equal. In order to interpret these data, Lax and Zeiger[33] report the results of a theoretical calculation of the line shape expected for a minority carrier in the presence of a majority carrier of the same sign. This curve resembles very closely the two dominant peaks for both the holes and electrons of Fig. 10. The remaining peaks in the experimental traces were then interpreted as harmonics. The presence of harmonics for the minority carriers appears quite convincing but perhaps less so for the majority carriers. They used the selection rules for such harmonics as developed from the Boltzmann theory for warped surfaces[19] and also used the symmetry properties of the graphite crystal to conclude that the energy surfaces corresponding to the carriers in graphite are warped ellipsoids with the major axis along the hexagonal [1000] direction and further, that the location of the overlapping bands in the hexagonal planes can be restricted to three possibilities near A as shown in Fig. 11. Recent theoretical work by McClure[34] has shown that position AB is the most likely and that the ellipsoids are indeed highly warped with the Fermi surface intersecting protrusions of the warped surfaces to give rise to the minority carriers. It should be mentioned that the de Haas-van Alphen experiments did not detect the presence of the minority carriers. However, results for the majority carriers are in good agreement with the cyclotron resonance data as indicated below.

The appearance of cyclotron resonance effects in tin and copper has been reported by Fawcett[35] who measured the resistance of the metal specimens calorimetrically. His samples were in the form of disks which were placed at the end of a square wave guide. The absorption of the microwave signal by the samples was measured by a very sensitive carbon composition thermometer attached to the outer face of the specimen. The resultant absorption or resistance curves as a function of magnetic field each showed a minimum and a

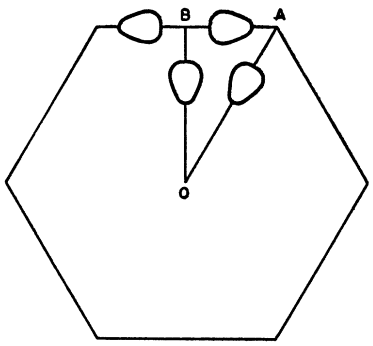

FIG. 11. Cross section of the Brillouin zone of graphite, with possible locations of band maxima and minima. Size of the energy contours is exaggerated. (After Lax and Zeiger.)

[32] Galt, Yager, and Dail, Phys. Rev. **103**, 1586 (1956).

[33] B. Lax and H. J. Zeiger, Phys. Rev. **105**, 1466 (1957).
[34] J. W. McClure, Phys. Rev. **108**, 612 (1957).
[35] E. Fawcett, Phys. Rev. **103**, 1582 (1956).

peak. He identifies the peaks as resonances, and gives mass values m^* from $0.23m_0$ to $0.43m_0$ for tin, and an estimate of $m^* \sim 1.5m_0$ for copper. He also reports anisotropy effects for both metals with orientation of magnetic field.

Azbel and Kaner[36] have predicted the existence of another form of cyclotron resonance which depends on the presence of the extreme anomalous skin effect in metals at low temperatures. Under these conditions, the mean free path is considerably larger than the penetration depth of the microwave field. In the Azbel-Kaner resonance, the magnetic field is oriented parallel to the surface and the electron, which moves in a helical orbit, returns to the "skin" at the surface each first, second, or third period depending on the magnetic field. If the mean free path l is long and $l \gg r \gg \delta$, where r is the radius of the cyclotron orbit and δ the effective skin depth, the electron will return several times in the proper phase to absorb energy resonantly at the fundamental frequency and at harmonic frequencies. The effect predicts oscillations with spacing proportional to $1/H$ for $\omega\tau \gg 1$. Experimentally this would be observed by looking for harmonic peak absorption at low magnetic fields at one-half, one-third, etc., of that for the fundamental. It is now believed that Fawcett's experiments[35] were the first to indicate the existence of this effect. Foner *et al.*[31] did report the peaks discussed above in bismuth at 4.2°K with the magnetic field parallel to the surface. Some of these did disappear when the magnetic field was tipped out of the surface. Some of the peaks shown in Fig. 9 may be associated with the Azbel-Kaner effect; however, this is not yet firmly established, since they have been observed by tracing the derivative of the absorption curve. If the absorption is genuine, it should also be observable with a sensitive absorption spectrometer. Recently, Kip[37] reported preliminary observations of the Azbel-Kaner resonance in tin with the magnetic field and the electric fields parallel to one another in the surface of the sample. Independently Aubrey and Chambers[38] also observed such a resonance, but in bismuth. The latter results were strikingly similar to the theoretical predictions and were obtained for both the surface resistance and reactance of the anomalous absorption at low temperatures, with the electric and magnetic fields in the plane of the sample parallel to each other.

Infrared Cyclotron Resonance

The microwave cyclotron resonance experiments, so highly successful in providing a fairly comprehensive picture of the bands in germanium and silicon, did not live up to expectations in other semiconductors. Even in the metals, bismuth and graphite, particularly in the latter where the results were relatively informative, the situation was not fully satisfactory from a quantitative point of view. The difficulties in the semiconductors, such as the intermetallic and polar compounds and semiconducting alloys, stemmed from the large scattering even at low temperatures, such that $\omega\tau < 1$. The purification of the compounds had not yet reached the state of perfection of germanium and silicon, resulting in large impurity scattering. In n-type indium antimonide and in metals, the presence of high carrier densities gave rise to depolarization or plasma effects. In essence, this meant that $\omega < \omega_p = (ne^2/m^*\epsilon)^{\frac{1}{2}}$, where ω_p is the plasma frequency, n the carrier density, m^* the effective mass, and ϵ the dielectric constant of the material. This situation is analogous to that in the ionosphere for a radio wave whose frequency is below cutoff. In the same way, the microwave field could not penetrate the metallic surface beyond the effective skin depth although $\omega\tau > 1$ for such materials as bismuth and graphite. The way out of this dilemma was to carry out experiments at millimeter and infrared frequencies. To get substantial improvement, the latter looked more attractive, since it could overcome the plasma effect in the semimetals. However, this poses a new problem. Even with small masses ($\sim 0.01m_0$ or somewhat larger), the substantial increase in frequency from 2.5×10^{10} to 3×10^{12} or 3×10^{13} made it necessary to use magnetic fields from 50 000 to several hundred thousand gauss, in order to reach resonance. Two approaches present themselves, namely using very large solenoids of the Bitter design, capable of providing dc fields up to $\sim$100 000 gauss, or using pulsed coils which can provide fields up to 10^6 gauss.

The initial infrared cyclotron resonance results were reported from the Naval Research Laboratory by Burstein, Picus, and Gebbie.[39] These experiments were carried out in a Bitter coil with an inner diameter of 4 in. whose peak field is about 60 000 gauss. The experiments were carried out with a prism spectrometer at a fixed wavelength of 41.1 μ where the absorption band of the atmosphere shows a gap. The magnetic field was set at a series of values over its range, and the signal was detected by a Golay cell. The infrared energy was either transmitted through a thin sample (20 μ) or reflected from the polished surface of a thick sample. Arrangements were made inside the coil to permit the magnetic field to be perpendicular or parallel to the surface. Figure 12 displays two sets of resonance curves obtained at room temperature for indium antimonide, one showing transmission and the other reflection. The mass deduced from these measurements of the electrons gave $m^* \approx 0.015m_0$.

The second scheme, using high-field pulsed coils, was carried out by the Lincoln group.[40] The magnetic field was generated by discharging a bank of condensers

[36] Azbel and Kaner, Soviet Phys. JETP **3**, 772 (1956).
[37] Kip, Langenberg, Rosenblum, and Wagoner, Phys. Rev. **108**, 494 (1957).
[38] J. E. Aubrey and R. G. Chambers, J. Phys. Chem. Solids **3**, 128 (1957).
[39] Burstein, Picus, and Gebbie, Phys. Rev. **103**, 825 (1956).
[40] Keyes, Zwerdling, Foner, Kolm, and Lax, Phys. Rev. **104**, 1805 (1956).

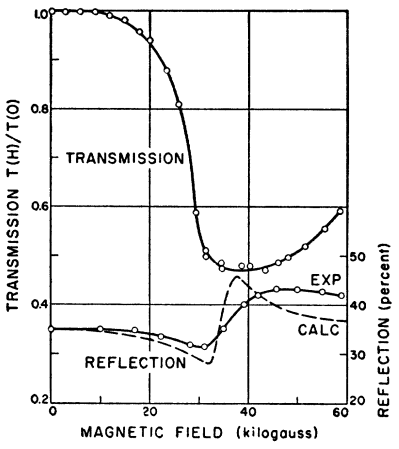

FIG. 12. Cyclotron resonance curves in InSb for both transmission and reflection as a function of magnetic field at a wavelength of 41.1 μ. Upper curve shows transmission through a 20-μ sample with magnetic field parallel to the surface. Lower solid line shows reflection from the surface of a 500-μ sample with magnetic field perpendicular to the surface. Theoretical curve (dashed line) calculated for $m^*=0.015m_0$ and $\omega\tau=16$. (After Burstein, Picus, and Gebbie.)

through specially built coils, having great mechanical strength. The discharge was triggered by a spark coil which initiated the breakdown of a spark gap in series with the condenser bank and the coil. The current through the coil produced a damped oscillatory field with a half-period of about 150 μsec. Observations were made during the first half-cycle. Use of pulsed fields of such short duration required the development of a sensitive infrared detector of fast response. This was achieved by the use of a 1-mm cube of zinc-doped germanium placed at the bottom of a hollow stainless-steel tube immersed in a helium bath. The tube contained dry helium, a parabolic mirror at the bottom which focused the infrared radiation onto the bottom surface of the germanium, and a suitable infrared window at the top. The infrared radiation was focused on the sample at the center of the coil whose inner diameter was $\sim\frac{3}{8}$ in. The signal passed through the specimen for transmission experiments or was reflected from a sample surface. The transmitted or reflected signal was then passed through a prism monochromator to the detector at a distance of about six feet to minimize electromagnetic pickup from the coil. Output of the detector was fed to a special circuit designed to reduce the time constant and over-all response of the detector to 2 μsec. The amplified signal was recorded by photographing an oscilloscope trace, triggered by light from the spark gap switch of the pulse magnet.

The initial transmission experiments were carried out at 12.7 μ with samples of indium antimonide and indium arsenide which were $\sim$200 μ thick, up to fields of 300 000 gauss. The traces showed broad absorption, as shown in Fig. 13, primarily due to dimensional broadening and perhaps also the apparent increase of the effective mass at higher magnetic field.† Since the samples were rather thick, the skin depth became less than that of the sample thickness as the magnetic field increased toward resonance. Thus, the signal was almost completely absorbed well below resonance, because the skin depth on resonance is of the order of 10 μ. Above resonance the skin depth remained less than that of the sample thickness until very high fields were reached, contributing further to the broadening of the resonance absorption. In order to eliminate this effect, reflection experiments were performed using polished surfaces, which were more easily prepared than the thin disks required for transmission. The resultant reflection traces are shown in Figs. 13(c) and 13(d). The value of the magnetic field for resonance is taken as the center of the steep portion of the reflection where it crosses the base line of the oscilloscope trace. This is then correlated with the calibrated trace shown in Fig. 13(e). From the known wavelength and value of the magnetic field on resonance the effective mass is determined. Figure 14 shows the plot of m^* *vs* B for InSb. The increase of m^* can be interpreted as evidence of the decreasing curvature of the band with energy. Similar results shown in Fig. 15 were also obtained for bismuth. In this case the samples were oriented such that the magnetic field was along $[11\bar{2}0]$ and $[10\bar{1}0]$ crystal directions. The mass values, which vary with magnetic field, correspond to

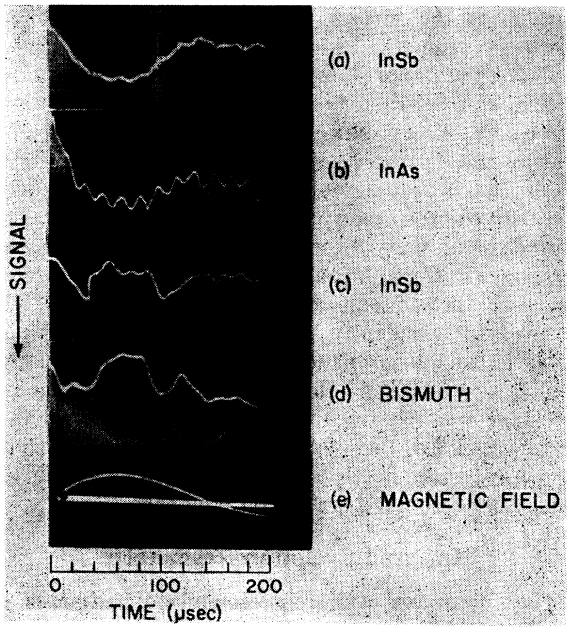

FIG. 13. Cyclotron resonance traces. Transmission signal through 200 μ samples at $\lambda=12.7$ μ: (a) InSb, $B_{max}=220$ kilogauss; (b) InAs, $B_{max}=155$ kilogauss; (c) InSb, (d) bismuth. Magnetic field trace *vs* time shown by curve (e). (After Keyes, Zwerdling, Foner, Kolm, and Lax.)

† Recently, R. J. Keyes has carried out transmission experiments with pulsed fields on thin InSb samples about seven microns thick and obtained resolvable resonance absorption which checks quite well with the reflection data.

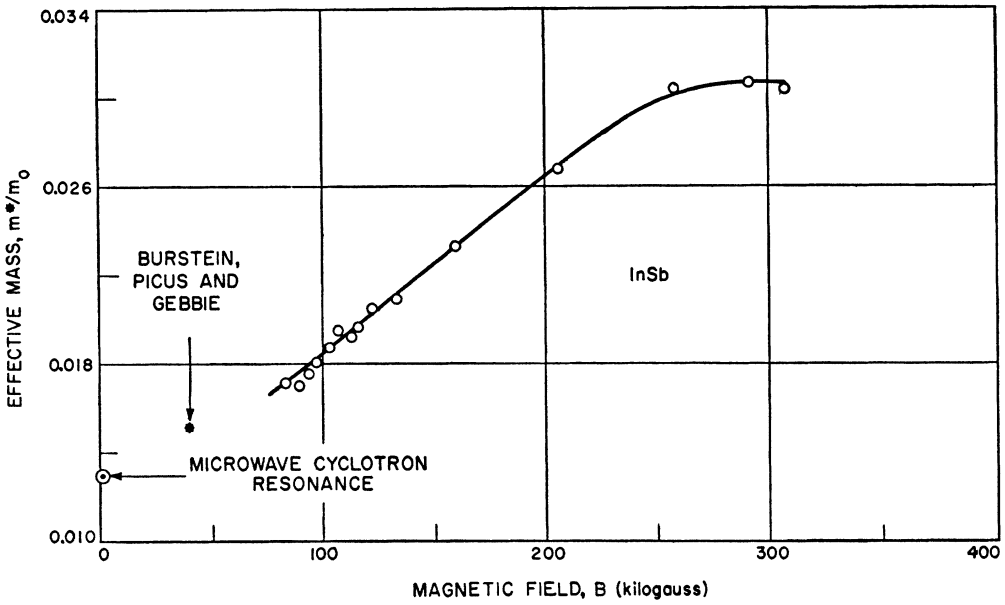

FIG. 14. Variation of effective mass with magnetic field in InSb from reflection experiments between $\lambda=10\,\mu$ and $\lambda=22\,\mu$. Magnetic field perpendicular to surface of sample. (After Keyes, Zwerdling, Foner, Kolm, and Lax.)

values of $0.009m_0$ along the [100] axis and $0.008m_0\bar{1}$ and $0.016m_0$ along the $[11\bar{2}0]$ direction for electrons as calculated from Shoenberg's de Haas-van Alphen data. One might consider the following explanation of the variation of the cyclotron resonance masses above and below the calculated values: The de Haas-van Alphen experiments are carried out at ~4°K and 1.2°K. The electrons which participate in the susceptibility measurements are those very close to the Fermi level. The infrared cyclotron measurements were carried out at 300°K resulting in the existence of unoccupied states corresponding to at least $kT\approx0.025$ ev below the Fermi level. The possibility has been considered that there are transitions at low magnetic fields between magnetic levels below the Fermi surface where the curvature of the band may be greater and hence m^* may be smaller. However, this must be ruled out from the results of the de Haas-van Alphen measurements in which there is obtained a linear relation between the position of the oscillation minima and maxima as a function of $1/H$. This is in good agreement with theory, indicating that the band is parabolic up to the Fermi level and the effective mass is independent of energy. Another, more likely explanation, is that the apparent effective mass is reduced by the plasma effect. Theoretically for the configuration used for the bismuth experiment and for the magnetic field perpendicular to the surface of the sample, the resonance field is determined by the relation

$$\omega_c/\omega\approx1-(\omega_p^2/\omega^2), \tag{10}$$

where $\omega_p=(ne^2/m^*\epsilon)^{\frac{1}{2}}$. Taking $n\approx10^{17}$ carriers per cm_8 for bismuth and $m^*\approx0.01m_0$ and ϵ equal to ϵ_0 for a metal since it has never been measured, this gives $\omega_p\approx2\times10^{14}$. At an infrared wavelength of $20\,\mu$, $\omega=10^{14}$/sec. Although this computation is approximate, it is apparent that this is a critical region where the formula of Eq. (10) predicts a departure from the normal resonance condition of $\omega_c=\omega$. This situation is particularly serious for small mass values and thus may account for the apparent mass values of cyclotron resonance below those obtained from the de Haas-van Alphen data. At high values of the resonance field where the effective masses are larger, a discrepancy cannot be accounted for by the plasma effect. At values of B greater than 75 000 gauss the lowest magnetic level is near to the Fermi level, hence transitions between it and the next higher level correspond to positions in the band of greater energy and lower curvature, resulting in smaller m^*. At very high fields the Fermi surface rises with the lowest magnetic level, which contains nearly all the electrons at room temperature.

Cyclotron resonance with pulsed magnetic fields has also been observed in InAs, zinc, and graphite. Quantitative results have been obtained in InAs yielding an electron mass $m^*\approx0.03m_0$ for fields between 150 000 and 250 000 gauss. At Lincoln Laboratory, experiments have also been carried out in the far infrared region ($81\,\mu$) on n-type InSb using KBr reststrahlen plates and dc magnetic fields of the order of 20 000 gauss.‡ Resonance curves similar to those of Fig. 12 using reflection have been obtained. The crossover of the reflection trace was observed at ~15 000 gauss giving an apparent effective mass of $\sim0.011m_0$. However, since this wavelength of $81\,\mu$ is approaching the critical wavelength of the plasma frequency corresponding to $126\,\mu$ for intrinsic InSb (as obtained from $\omega_p=(ne^2/m^*\epsilon)^{\frac{1}{2}}$ where $n\approx2\times10^{16}/cm^3$, $\epsilon\approx16$ and $m^*\approx0.013m_0$ from microwave cyclotron resonance), then it is necessary to make a correction. Theoretically, the crossover frequency under this condi-

‡ H. Lipson has extended these experiments to $93\,\mu$ and 29 000 gauss.

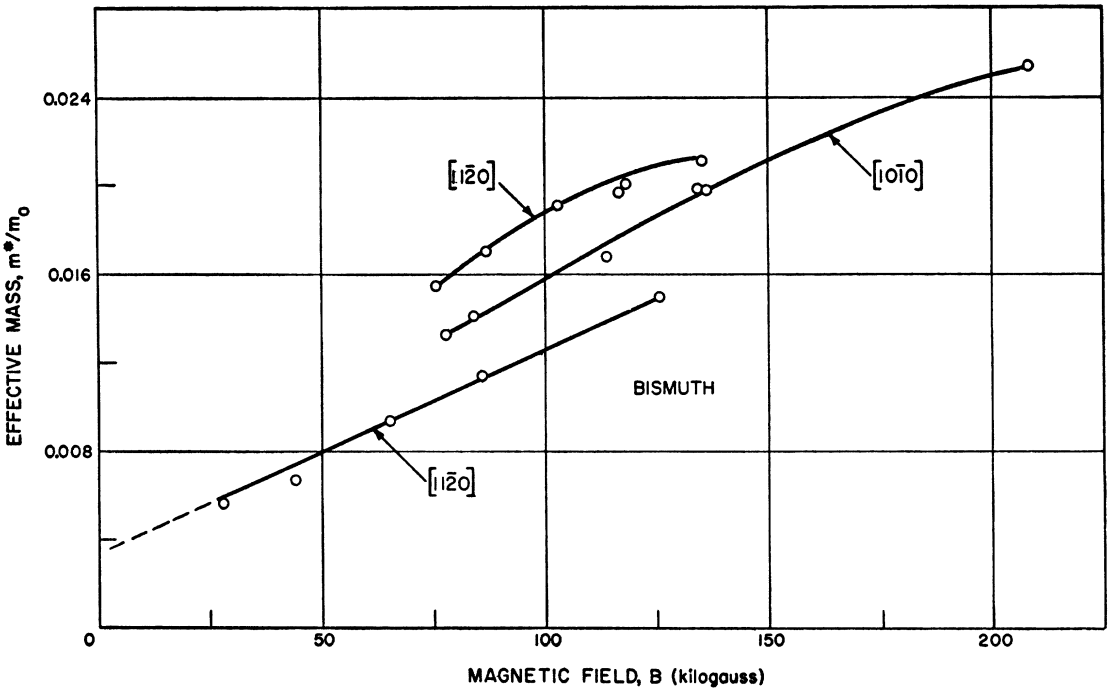

FIG. 15. Variation of effective masses with magnetic field in bismuth from reflection experiments. Magnetic field perpendicular to surface and parallel to the indicated crystal directions. (After Keyes, Zwerdling, Foner, Kolm, and Lax.)

tion is obtained from the relation

$$\omega_c/\omega \approx (1-\omega_p^2/\omega^2)^{\frac{1}{2}}.$$

Using the foregoing numerical values $\omega_c/\omega=0.76$. If the apparent mass is then corrected accordingly, one obtains $m^*\approx 0.014m_0$ which agrees well with the curve of Fig. 14.

DE HAAS-VAN ALPHEN EFFECT

In 1930, Schubnickow and de Haas[41] discovered that the magnetoresistance of bismuth at ~20°K exhibited an oscillatory behavior which was superimposed on the normal increase in the resistance as a function of magnetic field. Subsequently de Haas and van Alphen[42] observed the oscillatory effect of the diamagnetic susceptibility of bismuth at low temperatures as a function of magnetic field. This important phenomenon, known as the de Haas-van Alphen effect, was analyzed theoretically by Peierls,[43] Blackman,[44] and Landau.[45] The effect has now been observed in a large number of multivalent metals in addition to bismuth. Marcus observed the effect in zinc[46] and this has been studied subsequently in greater detail by other workers.[47] Shoenberg has reported experimental results of the de Haas-van Alphen effect in gallium, tin, graphite, cadmium, indium, antimony, aluminum, mercury, thallium, and lead.[48] A series of experiments was also carried out independently by Verkin, Lazarev, and Rudenko on tin, cadmium, beryllium, indium, magnesium antimony, and mercury[49] at about the same time. Recently, Berlincourt reported results in arsenic.[50]

Although the oscillatory behavior of the magnetic susceptibility has proved to be a useful tool for studying the fundamental properties of single crystals of metals in terms of their anisotropic behavior, other analogous oscillatory phenomena were also investigated. These effects have been observed in the study of magnetoresistance in bismuth[41] and later in other materials also. Oscillatory behavior of the Hall effect,[51] and the thermomagnetic effects[52] have also been discovered. Recently,

[41] L. Schubnikow and W. J. de Haas, Leiden Comm. No. 207d (1930).
[42] W. J. de Haas and P. M. van Alphen, Leiden Comm. No. 212A (1930).
[43] R. Peierls, Z. Physik **81**, 186 (1933).
[44] M. Blackman, Proc. Roy. Soc. (London) **A166**, 1 (1938).
[45] L. Landau, Proc. Roy. Soc. (London) **A170**, 341 (1939).
[46] J. A. Marcus, Phys. Rev. **71**, 559 (1947).
[47] B. I. Verkin and I. M. Dmitrenko, Bull. Acad. Sci. USSR **19**, 409 (1955); S. G. Sidoriak and J. E. Robinson, Phys. Rev. **75**, 118 (1949); L. Mackinnon, Proc. Roy. Soc. (London) **B62**, 170 (1949); F. J. Donaghoe and F. C. Nix, Phys. Rev. **95**, 1395 (1954).
[48] D. Shoenberg, Proc. Roy. Soc. (London) **A170**, 341 (1939); **A245**, 891 (1952); Physica **19**, 791 (1953).
[49] Verkin, Lazarev, and Rudenko, Doklady Akad. Nauk. SSSR **69**, 773 (1949); J. Exptl. Theoret. Phys. USSR **20**, 93 and 995 (1950); **21**, 658 (1951).
[50] T. G. Berlincourt, Phys. Rev. **99**, 1716 (1955).
[51] L. C. Brodie, Phys. Rev. **93**, 935 (1954); Reynolds, Leinhardt, and Hemstreet, Phys. Rev. **93**, 247 (1954).
[52] M. C. Steele and J. Babiskin, Phys. Rev. **94**, 1394 (1954); **98**, 359 (1955); J. Babiskin and M. C. Steele, Phys. Rev. **96**, 822 (1954).

Frederikse and Hosler,[53] in their study of the galvanomagnetic properties of InSb at low temperatures, have reported a discovery of an oscillatory effect in n-type material. Argyres[54] showed theoretically that this effect could occur in a semiconductor when it was degenerate. Since all of the oscillatory effects depend on the same basic phenomenon, we restrict the discussion to the de Haas-van Alphen effect. The information that relates the properties of the crystals to the band structure has been obtained by the study of the periodic nature of the magnetic susceptibility and not much new information has been added by other related phenomena. It must be mentioned, however, that greater accuracy has been achieved in some cases in recent measurements of the oscillatory magnetoresistance and Hall effect. Heretofore, the oscillatory phenomena in the galvanomagnetic and thermomagnetic properties have not been used for quantitative evaluation of effective masses because of the absence of a satisfactory theory. However, this situation may be rectified by the work of Zil'berman.[55]

Basic Phenomena

The basic phenomenon behind the oscillatory behavior of the electrical and magnetic properties of the various metals cannot be explained classically. The fundamental picture can only be described by quantum mechanics and is based upon the solution of the Schroedinger equation developed by Landau[56] for the motion of a free electron in a uniform magnetic field. The equation takes the form

$$-\frac{\hbar^2}{2m}\nabla^2\psi+\frac{\hbar\omega_c}{2j}\left(x\frac{\partial}{\partial y}-y\frac{\partial}{\partial x}\right)\psi+\frac{m\omega_c^2}{8}(x^2+y^2)\psi=\epsilon\psi, \quad (11)$$

where the magnetic field is along the z direction. Its solution can be reduced essentially to a simple one-dimensional harmonic oscillator. The resultant eigenvalues have a form which is similar to the harmonic oscillator, namely,

$$\epsilon_n=(n+\tfrac{1}{2})\hbar\omega_c+(\hbar^2k_z^2/2m),$$

where k_z is the component of the wave number along the magnetic field. Thus the energy levels in the two transverse dimensions $x-y$ are quantized with a spacing that is given by the cyclotron frequency and therefore proportional to the magnetic field. The number or density of energy states associated with each of these quantized levels also increases linearly with the magnetic field because the number of states in the band up to the Fermi level is equally divided between the Landau magnetic levels in $x-y$ plane and is given by $N_n\sim\hbar\omega_c/\epsilon_0$ for large n, where ϵ_0 is the height of the Fermi level above the bottom of the band. This effect, coupled with the increase in energy of the quantum or Landau level just above the Fermi level, gives rise to the oscillatory effects. When the energy of the Landau level exceeds that at the Fermi surface, the electrons drop into the adjacent level just below the Fermi level. When a level coincides in energy with the Fermi surface, the electrons in that level contribute a maximum effect to the susceptibility or conductivity. Thus, the peaks of these oscillations should correspond to the condition:

$$(n+\tfrac{1}{2})\hbar\omega_c=\epsilon_0. \quad (12)$$

This result can be obtained by considering the free energy of the electrons, using the appropriate partition function with the Fermi-Dirac statistics applied to the quantized system of levels. The second derivative of the free energy with respect to H gives the susceptibility whose oscillatory component in its simplest form is given by Landau's expression[45]

$$\chi=\sum\frac{Am'^{\frac{3}{2}}\epsilon_0}{m^{*2}T^{\frac{1}{2}}}\left(\frac{2\pi^2kT}{\beta H}\right)^{\frac{3}{2}}\times\exp\left(\frac{-2\pi^2kT}{\beta H}\right)\sin\left(\frac{2\pi\epsilon_0}{\beta H}-\frac{\pi}{4}\right), \quad (13)$$

where $\beta=e\hbar/m^*c$.

Thus the susceptibility has a sinusoidal behavior whose maxima are given by Eq. (12). The quantity m' is the density of states effective mass and m^* is the cyclotron resonance effective mass of Eq. (4). Furthermore, m^* depends on the direction of the magnetic field with respect to the crystalline axes if the surfaces are anisotropic. The anisotropy of the susceptibility provides a method for determining the parameters of the energy surfaces of the bands intersected by the Fermi surface. However, in order to obtain absolute values of the effective masses, it is necessary to study the amplitude of the oscillations, in addition to determining its periodicity. The latter measures the value of β/ϵ_0, while the former can be used to determine the value of β by comparing the amplitude at two different temperatures or from the slope of a suitable logarithmic plot of the amplitude with temperature. This has been the technique for the analysis of the experimental data using the approximate relation of Eq. (13). The more exact relations contain additional terms, associated with possible harmonics, and the exponential term is replaced by $1/(2\sinh)$. Dingle[57] has also shown that in order to take into account collision of electrons which lead to broadening of the oscillations, one has to add a parameter x to the temperature T in the exponential. Spin has also been neglected in this development. Despite these refinements the experiments have been carried out for the most part under conditions which are fairly well described by the simple expression given here.

[53] H. P. R. Frederikse and W. R. Hosler, Phys. Rev. **108**, 1136 (1957); Phys. Rev. **108**, 1146 (1957).

[54] P. N. Argyres, "Quantum theory of longitudinal magnetoresistance," Westinghouse Research Laboratory of Science Paper No. 6-94760-2-P6, Pittsburgh, Pennsylvania (March, 1957).

[55] G. E. Zil'berman, Bull. Acad. Sci. USSR **19**, 361 (1955); J. Exptl. Theoret. Phys. USSR **29**, 762 (1955).

[56] L. Landau, Z. Physik **64**, 629 (1930).

[57] R. B. Dingle, Proc. Roy. Soc. (London) **A211**, 517 (1952).

Experimentally it is necessary to go to low temperatures in order to obtain large amplitudes in the oscillations. From the exponential the term $\beta H \gtrsim 2\pi^2 kT$ for the oscillatory effect to be seen. Taking an effective mass of about $0.1m_0$ as a possible value to be measured, and $H \approx 30\,000$ gauss, it is necessary to go to 1°K to satisfy this condition. In order to observe a number of oscillations, it is necessary that $\beta H \ll \epsilon_0$, which is another requirement for the applicability of the approximate expression. Then the quantity β/ϵ_0 is determined from the periodicity of the oscillations. But for a spherical energy surface where $\epsilon = p^2/2m^*$, β/ϵ_0 is independent of the effective mass because

$$\epsilon_0 = \frac{h^2}{2m^*}\left(\frac{N}{V}\frac{8\pi}{3}\right)^{\frac{2}{3}} \tag{14}$$

and

$$\beta = e\hbar/m^*c,$$

where N/V is the number of electrons per cubic centimeter. Hence, in essence one determines in this case only the electron concentrations. In the monovalent metals, the noble metals and also copper, all of which have a large number of electrons in the conduction band, the value of ϵ_0 is large. These metals are also known to have effective masses of the order of unity. This means that the spacing between levels is very small and the number of levels is rather large. The situation from an experimental viewpoint is undesirable. The amplitude is small unless one uses very high fields of the order of $10^5 - 10^6$ to carry out experiments in the range of 4°K for $m^* \approx m_0$. This can be done but with some difficulty. The metals which have been examined with fields of the order of 10^4 gauss have given masses less than $0.1m_0$. Also the positions of the maxima of the susceptibility χ have been uniformly spaced as a function of $1/H$ with values of the order of 10^{-6} gauss^{-1}. This corresponds to N/V of the order of $10^{18} - 10^{19}$ per cc or $10^{-3} - 10^{-4}$ effective carriers per atom.

Experimental Techniques

In the original experiments of the de Haas-van Alphen effect, the Faraday force method was used. This involves the use of inhomogeneous magnetic fields which exert a force on the specimen to be measured. Usually the displacement of the sample is then measured by the deflection of a light beam. This method, although successful for observing the effect in bismuth, is inherently not suitable since the inhomogeneous field tends to smear out the rapid oscillations associated with masses larger than those found in bismuth. Consequently the method which has been adopted is that developed by Shoenberg,[48] which uses a homogeneous field and measures the torque exerted on a torsion wire or a filament which suspends the crystal specimen. The torque is determined by the deflection of a light beam from a mirror suspended with the specimen. For deflections of several degrees, it was necessary to compensate for the displacement of the orientation of the crystal either by turning the magnet or by using a stiffer suspension to reduce the deflection. Verkin and co-workers accomplished the same result by suspending their sample on a galvanometer filament and then restoring the zero position by sending a current through the galvanometer. From the known properties of the torsion wires or the galvanometer, the deflection or the restoring current was used to calculate the torque on the sample. This method measures the difference between the two susceptibilities in the plane perpendicular to the suspending axis. The usual procedure is to suspend the sample along one of the principal axes and to orient the magnetic field in the transverse plane at an angle θ with one of the other axes as shown in Fig. 16. In this case, the z axis can represent the trigonal axis of a bismuth, antimony, or arsenic crystal or the hexagonal axis of graphite, zinc, cadmium, or beryllium, and the x and y axes are the binary axes of these crystals. By varying the angle θ the anisotropy of the magnetic susceptibility can be studied in detail using an expression[48] similar to that of Eq. (13) for the torque C:

$$\frac{C}{H^2 \sin\theta \cos\theta} = \Delta\chi = \sum \frac{A\Delta m}{\rho}\left[\frac{\pi^2}{6}\left(\frac{k}{\epsilon_0}\right)^{\frac{1}{2}} - \frac{1}{T^{\frac{1}{2}}}\left(\frac{2\pi^2 kT}{\beta H}\right)^{\frac{1}{2}} \times \exp\left(-\frac{2\pi^2 kT}{\beta H}\right)\sin\left(\frac{2\pi\epsilon_0}{\beta H} - \frac{\pi}{4}\right)\right]. \tag{15}$$

C is the couple observed along the axis of suspension which is perpendicular to H, and θ is the angle defined in Fig. 16. ρ is the density; A is a constant given by

$$A = e^2\epsilon_0/H^2c^2\hbar(2k)^{\frac{1}{2}}m'^{\frac{1}{2}}. \tag{16}$$

m' is the density of states mass which for an ellipsoid

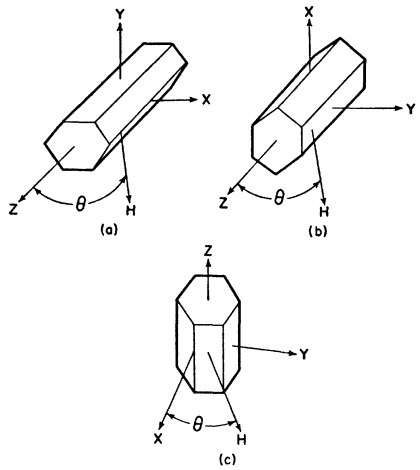

FIG. 16. Arrangement of crystals for de Haas-van Alphen experiments. Vertical axis is axis of suspension and the plane of the horizontal axes contains the magnetic field at a variable angle θ. The three principal modes of suspension are shown for a hexagonal crystal or for rhombohedral crystals like bismuth that have a trigonal and two binary axes.

having its axes aligned with the principal directions of the crystal would be given by $m'=(m_1m_2m_3)^{\frac{1}{3}}$. Δm is a factor involving the difference between the appropriate masses on the various ellipsoids taken along the x and y directions for each. The detailed expressions in the x, y, z coordinate system for the density of states mass m', the differential mass Δm, the cyclotron resonance mass m^* have to be determined for each ellipsoidal surface in terms of its mass tensor defined in this coordinate system, and for m^* also the angle θ of the magnetic field as given in Eq. (4). The first term in Eq. (15) is the steady part of the susceptibility and can also be anisotropic, since Δm appears. This anisotropy has been observed but has not been as useful for quantitative results as the analysis of the oscillatory component.

Another method has also been developed by Shoenberg.[58] The torque method, which uses homogeneous fields could not be extended to high fields above 30 000 gauss. Consequently high fields were produced by discharging a bank of condensers (1000 μf) charged to 1750 v through a coil in a liquid nitrogen bath. Peak fields of 100 000 gauss were obtained, homogeneous over a volume of 1 cm length and a few millimeters in diameter. Thin specimens of metal were immersed in a liquid helium bath inside the pulsed magnet coil. The sample was then surrounded by a small pickup coil, which was in series with another pickup coil used to balance out the emf induced in the measuring coil in the absence of the specimen. The first coil was used to measure the differential susceptibility dM/dH induced in the specimen during the pulse. The oscillatory effect was amplified and observed on an oscilloscope whose sweep was synchronized with the pulsed field. The periods of the oscillations were readily determined from the measurement of the peak field and the calibration of the time sweep of the scope. This method has been used to observe the effect for the first time in lead and was also used to study tin.

It is appropriate now to mention briefly the oscillatory Hall effect and magnetoresistance measurements. The Hall effect is studied by measuring the transverse field E_y induced in a sample in which the magnetic field **H** is along the z direction, and the electric field E_x is applied along the length of the specimen. The resistivity is studied as a function of the magnetic field intensity by measuring the value of the ratio of the current density J_x and E_x, i.e., $\rho=E_x/J_x$. The oscillatory component of both E_y and ρ is then observed at low temperatures superposed on the steady component of the galvanomagnetic measurements. The first oscillatory effects were observed by Shubnikov and de Haas[41] in bismuth. Such oscillations were recently correlated with the de Haas-van Alphen effect.[59] The experiments on the Hall effect and the thermomagnetic effects showed similar correlation.[51,52] The most recent work has been

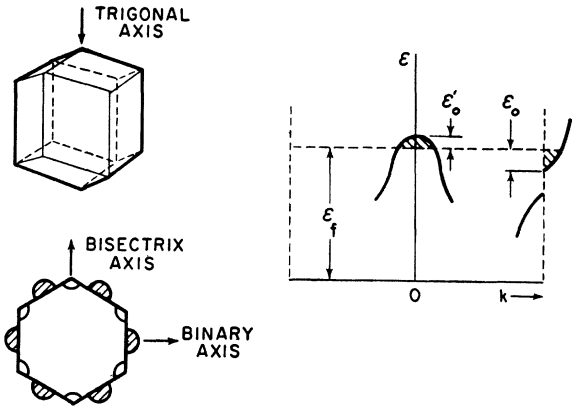

FIG. 17. Upper figure shows first Brillouin zone in bismuth. A cross section of the zone boundary transverse to the trigonal axis is shown in lower diagram. Shaded semicircles represent the field region in next outer zone which is occupied by electrons. One-dimensional diagram on the right is a simple schematic representing overlapping conduction and valence bands in bismuth.

carried out with fields up to 60 000 gauss by Babiskin[60] in bismuth. He observed oscillatory galvanomagnetic properties in a longitudinal magnetic field in which the current **I** was parallel to **H**. Other materials such as graphite, tin, zinc, and antimony have also shown similar correlation between the oscillatory behavior of their galvanomagnetic properties and the de Haas-van Alphen effect.

Experimental Results

Bismuth

Since bismuth has been studied extensively by three of the experimental methods treated here, it is appropriate to discuss its band structure in detail. Furthermore, some of its basic features are common also to antimony and arsenic which are also Group V metals and have rhombohedral crystal structure with a principal axis with trigonal symmetry, and three axes with binary symmetry. The first Brillouin zone for bismuth is shown in Fig. 17. The five valence electrons of bismuth are capable of filling this zone completely. However, some of the electrons overlap into the next higher zone, leaving an equal number of holes in the nearly filled zone. Bismuth is often referred to as a semimetal because it has overlapping bands. If for the present we follow the simple model first suggested by Jones[61] and later modified by Blackman,[44] we can account for the overlapping by assuming that an energy gap exists at the edge of the zone such that the overlapping electrons occupy the shaded minimum at the zone edge, with the Fermi level ϵ_0 above the bottom of this band. Then in momentum or k space the constant energy surfaces are six semiellipsoids, which combine from the opposite side to form actually three identical

[58] D. Shoenberg, Physica **19**, 791 (1953).
[59] P. B. Alers and R. T. Webber, Phys. Rev. **91**, 1060 (1953); T. G. Berlincourt, Phys. Rev. **91**, 1277 (1953).
[60] J. Babiskin, Phys. Rev. **107**, 981 (1957).
[61] H. Jones, Proc. Roy. Soc. (London) **144**, 225 (1934); **147**, 396 (1934).

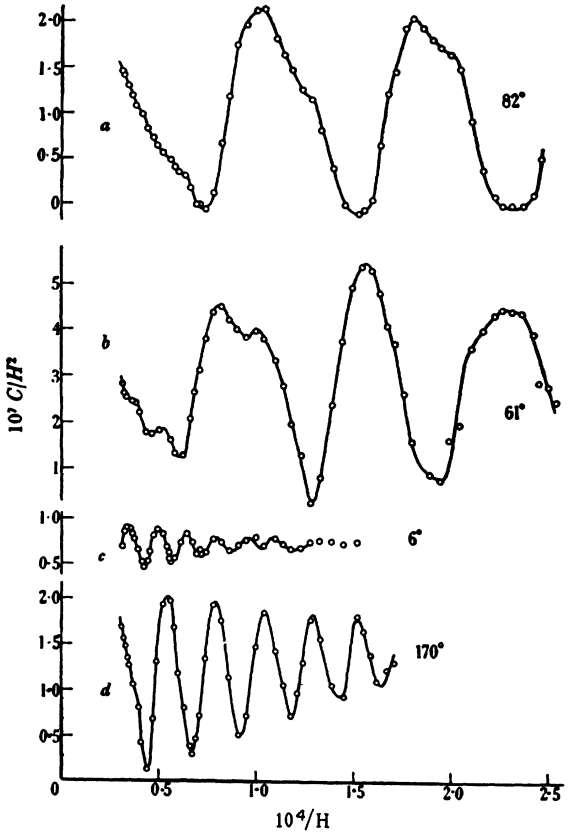

FIG. 18. Field variations of susceptibility, or actually C/H^2, for bismuth at 4.2°K for angles θ indicated at right. (a) and (b) suggest existence of two sets of oscillations or beats. (After Dhillon and Shoenberg.)

ellipsoids which are transformed into one another by a 120° rotation about the trigonal axis. The valence band is drawn at the center of the zone, in accordance with the latest speculations, and is shown to overlap the conduction band by a depth ϵ_0' above the Fermi level. The de Haas-van Alphen effect has given very little information as yet about the holes. For the electrons Shoenberg has shown that the three ellipsoids are really tilted out of the trigonal plane by about 6° for bismuth and that they can be represented by energy surfaces

$$2m_0\epsilon=\alpha_1 p_x^2+\alpha_2 p_y^2+\alpha_3 p_z^2+2\alpha_4 p_y p_z \qquad (17)$$

in the crystal coordinates which are then transformed into one another by a rotation of 120°. The mass tensor components are then related to the above parameters as

$$\frac{m_1}{m_0}=\frac{1}{\alpha_1},\quad \frac{m_2}{m_0}=\frac{\alpha_3}{\Delta},\quad \frac{m_3}{m_0}=\frac{\alpha_2}{\Delta},\quad \frac{m_4}{m_0}=-\frac{\alpha_4}{\Delta},\quad \Delta=\alpha_2\alpha_3-\alpha_4^2.$$

Using this model and applying it to Eq. (15), Dhillon and Shoenberg[62] analyzed a series of sweeps of the type shown in Fig. 18 for different values of θ for the three arrangements of suspension shown in Fig. 16. From the series of the oscillatory plots, those were chosen for detailed analysis which had only a single period left or in which one was predominant. From the plot of $1/H$ *versus* the quantum number for the maxima and minima as shown in Fig. 19, β/ϵ_0 was obtained from the selected orientations. To obtain β the amplitudes of the oscillations at two temperatures were compared, which for low quantum numbers are given by

$$\frac{T_2\sinh(2\pi^2kT_1/\beta H)}{T_1\sinh(2\pi^2kT_2/\beta H)}. \qquad (18)$$

By trial that value of β was selected which gave the best fit for the theoretical values of the ratio of Eq. (18) with the experimental values of ratios of the amplitudes for different values of $1/H$. From the different values of β the mass values m_1, m_2, m_3, and m_4 were determined. These values with other pertinent parameters are given in Table I as reported by Shoenberg.

Many other metals have been analyzed by Shoenberg and others in Russia. The data are summarized in Table I for all the materials. Some interesting features are shown by the results of Berlincourt[50] on arsenic, Verkin and Dmitrenko[47] on zinc, and those of Shoenberg[63] on gallium.

Arsenic

Arsenic has the bismuth crystal structure and therefore one would expect that the band structure would also be similar except for the numerical values of the masses. Berlincourt observed two sets of oscillations similar to Fig. 21. He studied the oscillatory curves for two modes of suspension (a) binary axis vertical and trigonal axis horizonal and (b) binary axis and trigonal axis horizontal. He analyzed both sets of curves in a manner analogous to that described before and determined the β/ϵ_0 values for each orientation from a plot similar to Fig. 19. The value of β was determined from the slope of an amplitude plot as a function of tempera-

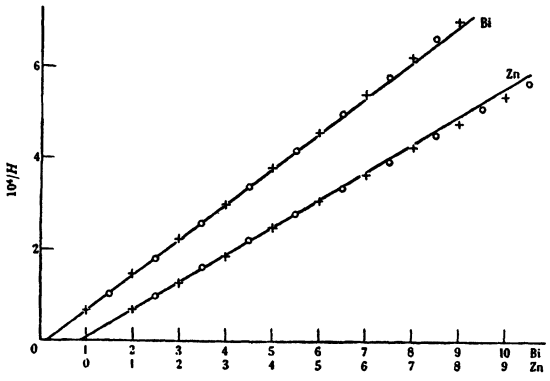

FIG. 19. Values of $10^4/H$ for maxima and minima plotted against successive half-integers for bismuth and zinc: 0, maxima; +, minima. (After Dhillon and Shoenberg.)

[62] J. S. Dhillon and D. Shoenberg, Phil. Trans. Roy. Soc. London **A248**, 937 (1955).

[63] D. Shoenberg, Proc. Roy. Soc. (London) **A245**, 891 (1952).

TABLE I. Electronic parameters of electrons and holes in semiconductors and metals.

A. Metals	Effective masses[a] m_1/m_0	m_2/m_0	m_3/m_0	m_4/m_0	Typical values of $\beta/\epsilon_0\times10^7$	$\epsilon_0\times10^{14}$ (erg)	n per atom	References
Cubic								
Al (a)	0.08				36	6		48
(b)	0.15				2.7	45		
Pb (a)	1.1				0.16	100	7×10^{-2}	
(b)	0.75				0.4	60	2.2×10^{-2}	48
Tetragonal								
Sn	0.10		2		2 to 6	31	1.5×10^{-3}	
In	0.3				2	29	1.7×10^{-3}	48
Orthorhombic								
Ga (a)	>0.2	>0.15	<0.05		20	10	$>0.3\times10^{-4}$	
(b)	0.1	0.3	0.03		30	11	0.4×10^{-4}	
(c)	0.2	0.02	0.4		50	6	0.7×10^{-4}	48
						Total	$>1.4\times10^{-4}$	
Hexagonal								
C (a)	3.6×10^{-2}		200		220	2.3	3.4×10^{-5}	48
(b)	7×10^{-2}		25 to 700		165	1.6	1.4 to 7×10^{-5}	
Holes	7×10^{-2}							
	2.8×10^{-2}							32, 33
Electrons	5×10^{-2}							
	1.5×10^{-2}							
Zn (a)	5.3×10^{-3}		0.2		700	4.9	0.9×10^{-6}	48
	1.6×10^{-2}	2.3×10^{-2}	2.5			1.6	6×10^{-6}	47
(b)	1.7	0.42	1.1×10^{-2}		2 to 20	7.2	2×10^{-4}	
Cd	0.4				2	23		
Tl	0.35				5 to 50	11	$\approx10^{-4}$	48
Be	0.03				70	8.4	3×10^{-6}	
Mg					19		7×10^{-5}	
Rhombohedral								
Bi †	2.4×10^{-3}	2.5	0.05	−0.25	200 to 800	2.9	1.5×10^{-5}	
Sb	0.05	1.00	0.52	−0.65	10 to 16	18	1.1×10^{-3}	48
Hg	0.15				10 to 14	9	$\approx10^{-4}$	
As (a)	3.1×10^{-2}	3.1×10^{-2}	0.23		300	1.59	1.5×10^{-6}	
(b)	0.193	1.07	1.78	−1.33	5	29.4	1.2×10^{-3}	50
†Bi	6.0×10^{-3}	1.0	2×10^{-2}	−0.10				38

B. Semiconductors		Effective masses[a] m_1/m_0	m_2/m_0	m_3/m_0	References
Ge	Holes	~0.3			8
		4.3×10^{-2}			
	Electrons	8.2×10^{-2}	8.2×10^{-2}	1.64	9, 15
		4.2×10^{-2}			128
Si	Holes	~0.5			14
		~0.17			
	Electrons	0.19	0.19	0.98	13
InSb	Holes	~0.2			25, 100
	Electrons	1.3 to 3×10^{-2}			25, 40
InAs	Electrons	3×10^{-2}			40

[a] In the cases of bismuth, tin, and arsenic, the masses m_1, m_2, m_3, and m_4 are the elements of the mass tensor $m=\begin{pmatrix} m_1 & 0 & 0 \\ 0 & m_2 & m_4 \\ 0 & m_4 & m_3 \end{pmatrix}$ in the coordinate system corresponding to the expressions for the energy surfaces in Eq. (17).

ture. The expression chosen for determining β was

$$\log_e\{aT^{-1}[1-\exp(-4\pi^2kT/\beta H)]\}, \qquad (19)$$

where a is the amplitude of the oscillation. The slope of this straight line for a given value of H should be equal to $-2\pi^2k/\beta H$. To a first approximation β was obtained from a slope of a plot of $\log_e(aT^{-1})$ *vs* T. This value of β was then used to plot the function of Eq. (19) giving a better approximation for β. The process was iterated to obtain an accurate value of β. Figure 20 shows the linear dependence of the function of Eq. (19) using the final values of β. The anisotropy results for the short period oscillations were interpreted in terms of the three tilted ellipsoids proposed for bismuth. The long period oscillations were interpreted in terms of a single ellipsoid. This was shown to be a fair approximation to the situation although it could not account for the presence of beats in the long period oscillations for some orienta-

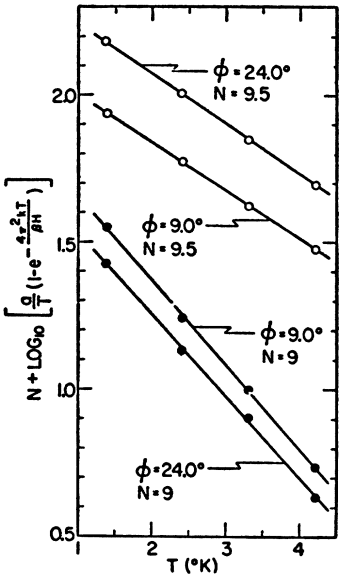

FIG. 20. Arsenic (pure). Temperature dependence of amplitude of de Haas-van Alphen oscillations for mode (b), binary and trigonal axes horizontal. Open circles correspond to long-period oscillations, and solid circles to short-period terms. Values of β derived from slopes of such plots. (After Berlincourt.)

tions. At present it appears that one set of carriers, perhaps the electrons, move on three tilted ellipsoidal surfaces at the zone edge if one draws an analogy with bismuth, and the holes move on a single ellipsoid of fairly small mass in the trigonal plane as shown in Table I.

Gallium

These experiments have been carried out for many metals, each with its own interesting features. Gallium is significant in that its band structure, which is fairly complicated, has apparently been untangled by Shoenberg[63] from the complicated de Haas-van Alphen oscillations obtained for gallium. Many of these curves show the presence of beats. These have been essentially separated by selecting the most suitable orientations of the crystal in which the beat structure became relatively simple like that of Fig. 21(b). Gallium is an orthorhombic crystal with three unequal axes. By choosing three sets of energy ellipsoids with their principal axes along these three crystalline axes in order to satisfy the symmetry properties of the crystal Shoenberg was able to obtain approximate values of the mass parameters representing this complicated structure. These values are given in Table I.

Zinc

Verkin and Dmitrenko[47] made a careful detailed study of the de Haas-van Alphen effect. They measured the couple acting on the zinc crystal with (a) one binary axis and the hexagonal axis in the horizontal plane and (b) the other binary axis and the hexagonal axis horizontal as shown in Figs. 21(a) and (b), respectively. Again low-frequency oscillations with large amplitude were observed. However, two high-frequency oscillations of smaller amplitude were also observed, as indicated by the graph of Fig. 21, which shows the high-frequency oscillations with a distinct beat in the curve marked (a). The procedure of analyzing the individual traces for the various orientations of the magnetic field in the two modes of suspension was followed, yielding the appropriate values of β/ϵ_0. The results are shown in the interesting plot of Fig. 22 in which is shown the anisotropy of the period of oscillations of the differential

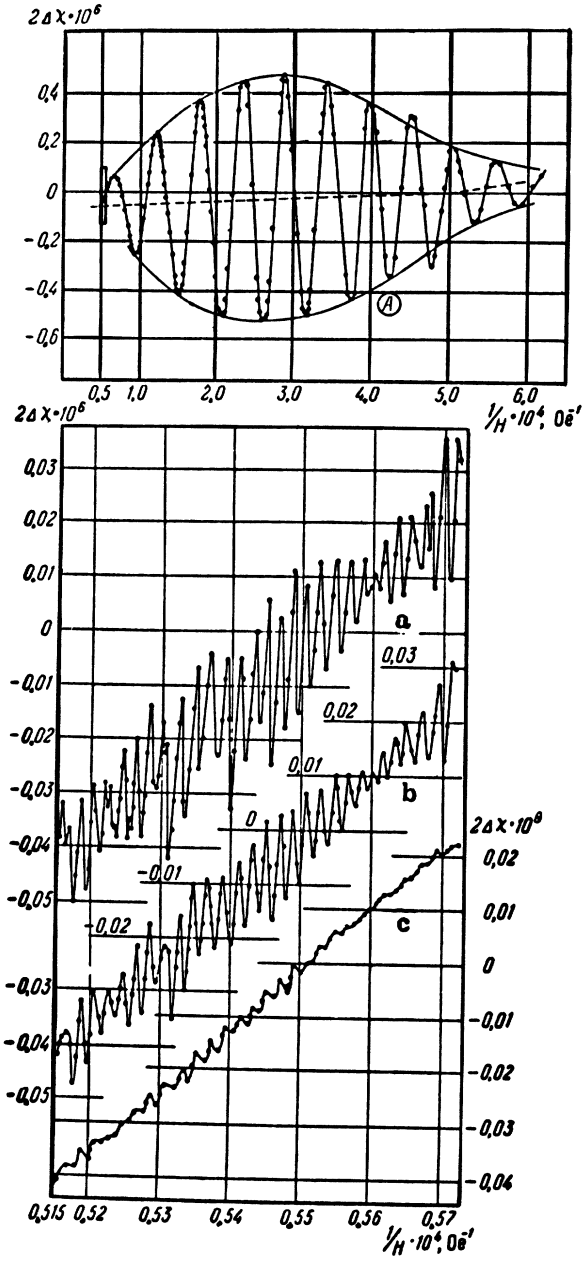

FIG. 21. Variation of differential susceptibility, $\Delta\chi$, of a zinc crystal in orientation (a) of Fig. 14 and $\theta=25°$. (A) 4.2°K, (a) 1.45°K, (b) 2.0°K, (c) 4.2°K. Curve *c* represents an enlarged (both coordinates) plot of the section of *A* enclosed in the rectangle; curves *a* and *b* are for the same $1/H$ interval as *c* but lower temperatures. (After Verkin and Dmitrenko.)

susceptibility as a function of angle for the two modes of suspension of the crystal. From the study of the anisotropy of the susceptibility of the crystal when it is suspended by the hexagonal axis it is evident that the magnetic properties possess trigonal symmetry. With this assumption in mind the theoretical expression for the couple or the susceptibility of Eq. (15) was expressed in terms of three sets of ellipsoids which transform 120° into one another about the hexagonal axis and with their principal axes parallel and perpendicular to the hexagonal axis. The analysis was carried out for the low-frequency component and for one of the high-frequency oscillations. The resultant mass values and related parameters for each are given in Table I.

In presenting these results for the de Haas-van Alphen effect, techniques and interpretation for obtaining the principal features of the band structure have been stressed. Some of the fine points of both the theoretical results and their application to the experiments have not been discussed. A discrepancy exists between the theoretical and experimental values of the phase constant δ in the oscillatory term $\sin(2\pi\epsilon_0/\beta H-\delta)$ of Eqs. (13) and (15). The theoretical value is taken as $\pi/4$ but the experiments give results that differ from this for many metals. No satisfactory explanation exists. Another phenomenon not treated here is the presence of harmonics for which both the theoretical and experimental situations are still unsatisfactory.

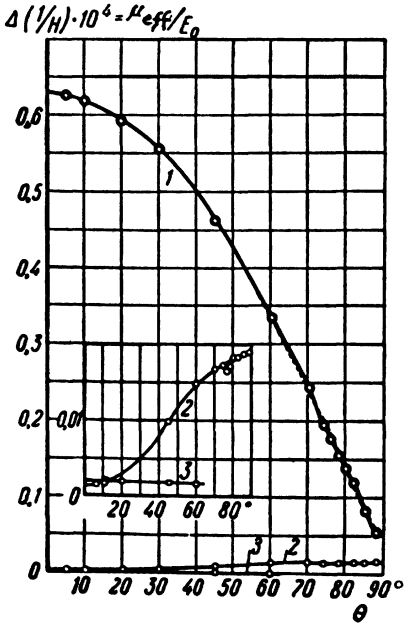

FIG. 22. Variation of period of oscillation of the differential susceptibility, $\Delta\chi$, of the zinc crystal in orientation (b) of Fig. 14 at 2.4°K and as a function of θ. (1): fundamental (low-frequency) component, (2) and (3): high-frequency components. (After Verkin and Dmitrenko.)

GALVANOMAGNETIC EFFECTS

The galvanomagnetic properties of many metals had been investigated in the past with some of the measurements on polycrystalline material. The most extensive work has been that of Kapitza[64] who measured the magnetoresistance of a large number of metals in magnetic fields up to 300 000 gauss and temperatures down to liquid air. The use of liquid helium temperatures and moderate values of magnetic fields of the order of 10^4 gauss[65] accomplished the same effect as that of the very high fields and higher temperatures. Many investigators carried out similar experiments subsequently which have been interpreted semiquantitatively on simple models of one or two carrier systems in which the anisotropy properties of the crystals were not taken into account. This situation was perhaps appropriate for explaining the results in polycrystalline materials but inadequate for single crystals. In particular the existence of longitudinal effects in the magnetoresistance could not be explained by the simple isotropic two-carrier model. Perhaps the single exception was the work of Jones,[66] who attempted to interpret the galvanomagnetic effects in bismuth in terms of spheroidal energy surfaces consistent with the crystalline symmetry of bismuth. However, not until recently were sufficiently precise experiments carried out on single crystals to allow quantitative analysis in terms of the detailed nature of the band structure. This recent work on semiconductors and metals is discussed in this section.

Germanium and Silicon

Perhaps the first detailed precise measurements that illustrate the usefulness of galvanomagnetic measurements for investigating the band structure of crystals were carried out by Pearson and Suhl.[67] They made an extensive study of the magnetoresistance of germanium at 300°K and 77°K as a function of crystal orientation. They cut specially shaped samples from large single crystal ingots along either [100] or [110] directions. The two end electrodes and four side electrodes which were part of the germanium samples were electroplated to provide good ohmic contact for the current and potentiometer leads. Current of the order of one milliampere was passed through both n- and p-type samples and the voltage drop (usually not in excess of one volt) was measured with a potentiometer across the side electrodes, with and without magnetic fields. In this way the magnetoresistance was measured up to values of about 20 000 gauss for different orientations of the crystal in the field. A few measurements were also taken on n-type samples oriented along the [100] direction in fields up to 100 000 gauss. The results which are pertinent here are shown in Fig. 23 for germanium. Figure

[64] P. Kapitza, Proc. Roy. Soc. (London) **123**, 292 (1929).
[65] W. Meissner and E. Scheffers, Physik *Z.* **30**, 827 (1929); L. Schubnikov and W. J. de Haas, Leiden Comm. No. 207 (1930).
[66] H. Jones, Proc. Roy. Soc. (London) **A155**, 653 (1936).
[67] G. L. Pearson and H. Suhl, Phys. Rev. **83**, 768 (1951).

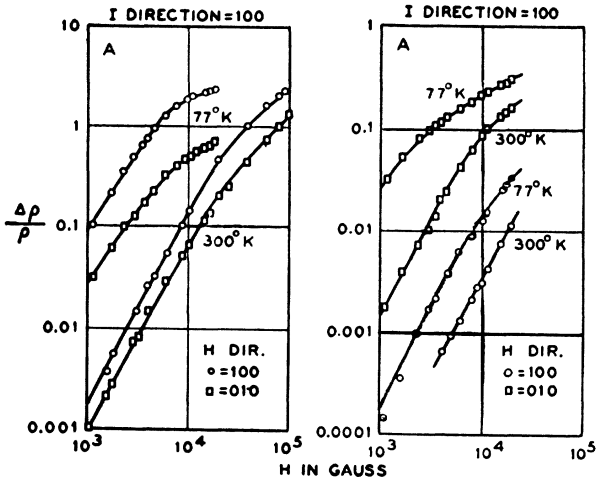

FIG. 23. $\Delta\rho/\rho$ *vs* H in germanium for fixed directions of **I** and **H** as indicated. Figure on left is for n type and on right is for p type. (After Pearson and Suhl.)

23 shows the change in resistance $\Delta\rho/\rho=(\rho-\rho_0)/\rho_0$ with magnetic field where ρ is the resistivity for any value of H and ρ_0 the value with $H=0$. For n-type material the transverse magnetoresistance is smaller than the longitudinal with the current I along the [100] direction. In the p-type material the transverse magnetoresistance always exceeded the longitudinal. The presence of the longitudinal magnetoresistance indicates the existence of anisotropic surfaces. Figures similar to Figs. 24 and 25 were obtained for fixed values of the magnetic field H and the temperature. The magnetic field was set at 4000 gauss in a horizontal direction and the sample mounted to rotate about a vertical axis, either about its length, width, or thickness, with the current always along the length, which was either a [100] or a [110] axis.

The interpretation of the anisotropy results for n-type germanium was given by Meiboom and Abeles[68] and

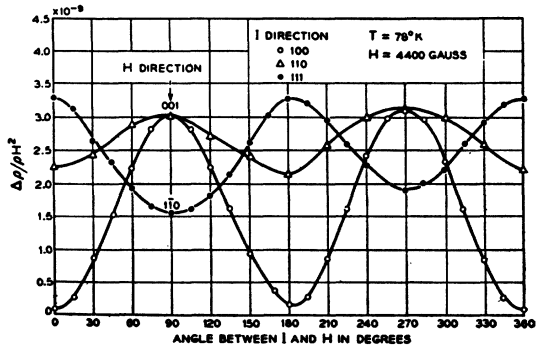

FIG. 24. Variations of $\Delta\rho/\rho H^2$ as **H** is rotated with respect to **I** in n-type silicon. Certain cardinal directions of **H** are indicated. The fixed directions of **I** and the temperature are given. (After Pearson and Herring.)

for p-type material by Lax and Mavroides.[69] In order to make quantitative interpretation of the magnetoresistance, Meiboom and Abeles assumed that the relaxation time $\tau=l\epsilon^{-\frac{1}{2}}$ where ϵ is the energy of the electron and l is a constant. They assumed that the energy surfaces were either three ellipsoids of rotation along the [100] axes or four ellipsoids of revolution along the [111] axis, both arrangements being consistent with the cubic symmetry of the crystal. The first model can be eliminated from simple arguments as follows: The experimental results for n-type germanium indicate a large longitudinal magnetoresistance along the [100] direction. If the ellipsoids had their principal axes along this direction, the electrons would behave essentially as isotropic carriers, with appropriate effective masses for each ellipsoid. This happens because the

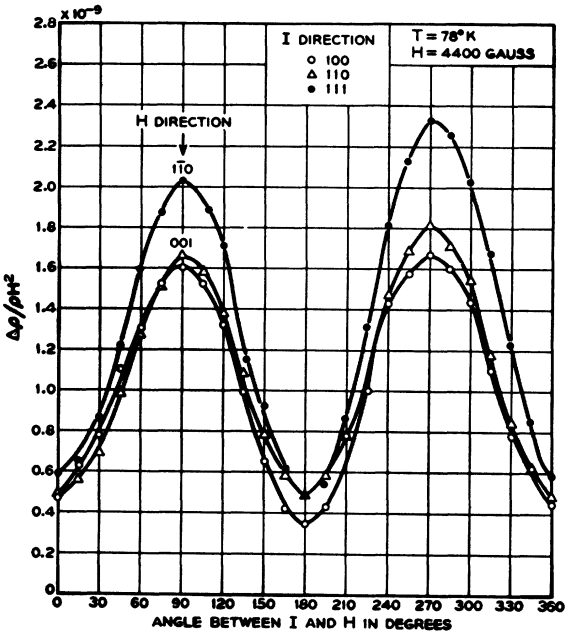

FIG. 25. Variations in $\Delta\rho/\rho H^2$ as **H** is rotated with respect to **I** in p-type silicon. (After Pearson and Herring.)

electrons rotate about the magnetic field in a plane perpendicular to **H**. Consequently, the current along the magnetic field remains unaffected by **H**. However, when the ellipsoids are along the [111] direction and the magnetic field along the [100] direction, then since **H** is tilted relative to the principal axes of the ellipsoid, the motion of the electron due to **H** is no longer perpendicular to it. Consequently, the component along **H**, will be responsible for the existence of a longitudinal magnetoresistance. Using this model, Meiboom and Abeles calculated the current component i_i for each ellipsoid as a series expansion in H:

$$i_i=\sigma_{ik}E_k+\sigma_{ikl}E_kH_l+\sigma_{iklm}E_kH_lH_m+\cdots, \quad (20)$$

[68] S. Meiboom and B. Abeles, Phys. Rev. **93**, 1121 (1954); B. Abeles and S. Meiboom, Phys. Rev. **95**, 31 (1954).

[69] B. Lax and J. G. Mavroides, Phys. Rev. **100**, 1650 (1955); J. G. Mavroides and B. Lax, Phys. Rev. **107**, 1530 (1957).

where

$$\sigma_{ik}=-\int a\tau\frac{\partial f_0}{\partial\epsilon}\frac{\partial\epsilon}{\partial p_i}\frac{\partial\epsilon}{\partial p_k}dV$$

$$\sigma_{ikl}=ab\int\tau\frac{\partial f_0}{\partial\epsilon}\frac{\partial\epsilon}{\partial p_i}\frac{\partial\epsilon}{\partial p_r}\frac{\partial}{\partial p_s}\left(\tau\frac{\partial\epsilon}{\partial p_k}\right)\epsilon_{lrs}dV$$

$$\sigma_{iklm}=-ab^2\int\tau\frac{\partial f_0}{\partial\epsilon}\frac{\partial\epsilon}{\partial p_i}\frac{\partial\epsilon}{\partial p_r}\frac{\partial}{\partial p_s}\times\left[\tau\frac{\partial\epsilon}{\partial p_t}\frac{\partial}{\partial p_\mu}\left(\tau\frac{\partial\epsilon}{\partial p_k}\right)\right]\epsilon_{mrs}\epsilon_{lt\mu}dV$$

$$a=e^2/4\pi^3\hbar^3,\quad b=e/c,$$

where the restriction on the conductivity tensor components σ_{ik}, σ_{ikl}, σ_{iklm} and also on the unity factor ϵ_{lrs}, etc., reduce their number to those satisfying cubic symmetry for the system. E_k, H_l, and H_m are the components of the electric and magnetic fields respectively, τ the collision time which is a function only of ϵ, the energy, p_i the component of momentum, f_0 the distribution function which is taken as the Boltzmann distribution, and dV the volume element in momentum space. Using these assumptions, each of the conductivity coefficients was evaluated in the ellipsoidal coordinate system up to the H^2 term using the integrals of Eq. (20). The total current density J_i was then evaluated by transforming the conductivity coefficients of each of the four ellipsoids to the cubic coordinate system and summing the coefficients for all the ellipsoids. The galvanomagnetic coefficients were obtained by inverting a relation similar to that of Eq. (20) but between J_i and E_k, giving the following results[68]:

$$\begin{aligned}R_0&=(3\pi/8)[3K(K+2)/(2K+1^2](1/Nec)\\ M_{100}/H^2&=(8/3\pi)R_0^2\sigma_0^2(2K+1)(K-1)^2/K(K+2)^2\\ M_{100}{}^{010}/H^2&=(1/3\pi)R_0^2\sigma_0^2[K^2(16-3\pi)\\ &\quad+K(16-6\pi)+4]/K(K+2)\\ M_{110}&=(1/2)M_{100}\quad M_{110}{}^{001}=M_{100}{}^{001}\\ M_{110}{}^{1\bar{1}0}&=(1/2)M_{100}+M_{100}{}^{010},\end{aligned}\tag{21}$$

where R_0 is the Hall coefficient; σ_0 the conductivity; N the total number of electrons in the conduction band; $M_{ikl}/H^2=(\sigma_0-\sigma)/\sigma H^2$ the longitudinal magnetoresistance in the (ikl) direction; and $M_{ikl}{}^{mnp}/H^2$ the transverse magnetoresistance with the current **I** along the (ikl) direction and **H** in the (mnp) direction. Using the foregoing expressions and $K=20$, Abeles and Meiboom made a good fit of the data of Pearson and Suhl at 300°K and 77°K as shown in Table II. In this way Meiboom and Abeles independently predicted ellipsoids along the [111] direction for electrons in germanium in good agreement with the results of the Lincoln group[9] from cyclotron resonance. They also carried out a calculation for strong fields, in addition to the low field expansion discussed here, and obtained good agreement of the dependence of the magnetoresistance as a function of magnetic field using the experimental data of Fig. 23 and $K=20$.

TABLE II. Comparison between measured and calculated magnetoresistance coefficients (in gauss^{-2}) of n-germanium at low magnetic field strengths.

Direction		$(\sigma_0-\sigma)/\sigma H^2$			
I	H	300°K calc	300°K exp	77°K calc	77°K exp
100	100	1.91×10^{-9}	1.92×10^{-9}	87.2×10^{-9}	88×10^{-9}
100	010	0.91	0.90	41.4	28.5
110	001	0.91	1.03	41.4	31.5
110	$1\bar{1}0$	1.86	1.68	85.0	75
110	110	0.95	0.99	43.6	58

Magnetoresistance experiments on single crystals of silicon similar to those described for germanium were carried out by Pearson and Herring.[70] Rods were cut with their lengths along the [100], [110], and [111] directions. Resistivity measurements at zero field and at 4400 gauss were made and the sample was rotated in the magnetic field about its width axis which was perpendicular to **H**. Hall measurements were made simultaneously with the current perpendicular to the magnetic field. The results of the experiments are shown in Figs. 24 and 25 for n-type and p-type silicon, respectively, at 78°K. The longitudinal magnetoresistance for n-type material along the [100] direction is small but the transverse magnetoresistance with **I** along [100] is large. In the [110] direction the two are comparable with the transverse slightly larger. However in the [111] sample the longitudinal magnetoresistance is larger by a factor of 2 than the transverse. Based upon the nearly vanishing longitudinal magnetoresistance along the [100] direction, Pearson and Herring suggested that the energy surfaces consisted of six ellipsoids along the [100] axes corresponding to six minima along these directions somewhere between the center and edge of the Brillouin zone. Using an analysis similar to that of Meiboom and Abeles, they deduced that the mass ratios of the ellipsoids $K=m_l/m_t$ were as follows: at $T=68$°K, $K=4.6$ and $T=298$°K, $K=4.9$. These values are in good agreement with the value $K=5$ determined from cyclotron resonance.[13]

Theoretical work on the galvanomagnetic effects in cubic semiconductors with spheroidal energy surfaces was also carried out by Shibuya[71] who used his results to explain the galvanomagnetic effects in germanium. Following the cyclotron resonance results, a phenomenological theory for the galvanomagnetic effects using the ellipsoidal models for germanium and silicon was worked out by Herring[72] and Herring and Vogt.[73] Detailed calculations were made by Gold and Roth[74] with the

[70] G. L. Pearson and C. Herring, Physica **20**, 975 (1954).
[71] M. Shibuya, Phys. Rev. **95**, 1385 (1954).
[72] C. Herring, Bell System Tech. J. **34**, 237 (1955).
[73] C. Herring and E. Vogt, Phys. Rev. **101**, 944 (1956).
[74] L. Gold and L. M. Roth, Phys. Rev. **103**, 61 (1956).

approximation of an energy-independent τ. Their results showed many of the anisotropy features for n-type germanium and silicon similar to those shown in Fig. 24. Glicksman[75] considered the galvanomagnetic properties of semiconductors having two sets of ellipsoidal energy surfaces: one set along the [100] direction and the other set along the [111] direction. His analysis was particularly applicable to Ge-Si alloys.

Experiments on the Hall effect on oriented single crystals of n-type germanium were carried out by Bullis and Krag[76] and the anisotropy results correlated with the phenomenological theory using the data of the cyclotron resonance experiments. Bullis[77] carried out extensive experiments on the magnetoresistance of n-type germanium as a function of impurities and also as a function of temperature. From the longitudinal magnetoresistance along the [100] direction, he obtained values of the mass ratio K which depended on temperature and impurity concentration. He obtained mass ratios smaller than 20 that decreased with temperature and resistivity. These estimates were based on the existing theories which assume that $\tau = l\epsilon^n$ where n has the appropriate numerical value. He concluded that since the galvanomagnetic measurements actually measure mobility which is proportional to τ/m^*, his apparent change in mass was a result of the anisotropy of scattering of an electron moving on an ellipsoid. Thus he demonstrated that the galvanomagnetic measurements give qualitative or at best, semiquantitative information regarding the band structure. Similar results of the variation of the mass ratio were obtained by Benedek, Paul, and Brooks[78] in their study of n-type germanium as a function of pressure. They interpreted their change in mass ratios due to pressure as a change in the curvature of the band as function of pressure. However, it is possible that their results are also influenced by anisotropic scattering. Glicksman and Christian[79] also obtained smaller mass ratios in Ge-Si alloys containing small percentages of silicon and attributed these to anisotropic scattering. Recently, Goldberg[80] and Broudy and Venables[81] have also suggested that there exists anisotropic scattering in n-type germanium.

The first quantitative work on p-type germanium was carried out by Willardson, Harman, and Beer[82] who used the simple two carrier model and the average effective masses of holes (obtained from cyclotron resonance) to account for the behavior of the transverse Hall and magnetoresistance coefficients as a function of magnetic field and temperature. They calculated the coefficients assuming lattice scattering or a mean free path independent of the electron energy at a given temperature. A typical result is shown in Fig. 26. The large reduction of these galvanomagnetic coefficients for values of the magnetic field of the order of 7000 gauss was attributed to the presence of the small hole since the radius of its magnetic orbit was reduced to a very small value at high values of the magnetic field. Then the contribution to the electrical properties of the material is negligible. Experiments and analysis of magnetoconductivity in p-type germanium has also recently been reported by Goldberg, Adams, and Davis.[83] Their theoretical work also involved the use of a simple two carrier model.

In order to explain the anisotropy data and the galvanomagnetic properties of p-type material, Lax and

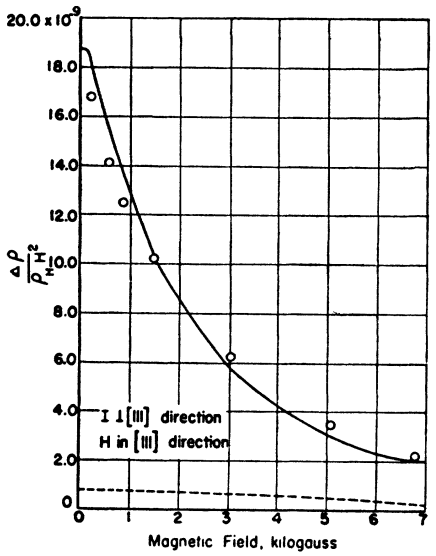

FIG. 26. $\Delta\rho/\rho_H H^2$ *vs* H for a p-type germanium specimen. The experimental points were taken at 205°K. The solid line was calculated using Hall data. Dashed line is calculated behavior when only heavy hole is taken into account. (After Willardson, Harman, and Beer.)

Mavroides[69] developed a scheme for evaluating the conductivity coefficients of Eq. (20) using the energy momentum relation of Eq. (5) obtained from cyclotron resonance. The energy-momentum relation was expressed in spherical coordinates and then the radical of Eq. (5) was expanded appropriately in a form that gave a rapidly converging series whose higher order terms were neglected. The choice of the spherical coordinates and additional expansion of the spherical harmonics permitted evaluation of the coefficients of Eq. (20). In this way expressions for the density of states, conductivity, Hall and magnetoresistance coefficients were obtained involving a series expansion of the anisotropy parameters associated with the surface. The results were applied to the analysis of Hall data, magneto-

[75] M. Glicksman, Phys. Rev. **102**, 1496 (1956).
[76] W. M. Bullis and W. E. Krag, Phys. Rev. **101**, 580 (1956).
[77] W. M. Bullis, Doctoral thesis, Department of Physics, Massachusetts Institute of Technology (1956).
[78] Benedek, Paul, and Brooks, Phys. Rev. **100**, 1129 (1955).
[79] M. Glicksman and S. M. Christian, Phys. Rev. **104**, 1278 (1956).
[80] C. Goldberg, Bull. Am. Phys. Soc. Ser. II, **2**, 65 (1957).
[81] R. M. Broudy and J. D. Venables, Phys. Rev. **105**, 1757 (1957).
[82] Willardson, Harman, and Beer, Phys. Rev. **96**, 1512 (1955).
[83] Goldberg, Adams, and Davis, Phys. Rev. **105**, 865 (1957).

resistance, and the variation of the energy gap in germanium and silicon. The analysis of the energy gap as a function of temperature using experimental data of Morin and Maita[84] gave the results shown by the dashed lines shown in Fig. 27. The solid curves are those of Macfarlane and Roberts[85] obtained from infrared absorption data discussed later. The important result is that two sets of curves were chosen for germanium by assuming that there were either four or eight ellipsoids. The curve with 4 ellipsoids was in much better agreement with the infrared data. This indicates that the conduction band minima occur at the edge of the zone. This is consistent with the data of Crawford, Schweinler, and Stevens[86] obtained from magnetic susceptibility measurements in n-type germanium. Similarly for silicon three and six ellipsoidal models were compared with the infrared data and the six ellipsoidal model was in closer agreement. This was predicted theoretically and agrees with the conclusions drawn by Macfarlane and Roberts[85] from their interpretation of the infrared experiments.

Mavroides and Lax[69] also used their results to explain

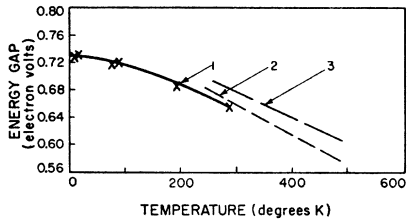

FIG. 27. Variation of energy gap in germanium with temperature. (1) data of Macfarlane and Roberts; (2) Lincoln Laboratory calculations for 4-ellipsoid model; and (3) Lincoln Laboratory calculations for 8-ellipsoid model. (After Lax and Mavroides.)

the anisotropy of the magnetoresistance data of Figs. 23 and 25 in p-type material using a suitable approximate value of the scattering time τ for τ independent of ϵ and constant mean free path. The comparisons of theory and experiment are shown in Table III showing good agreement with the exception of the M_{100} coefficient.

Bismuth

The model developed by Jones[66] for the galvanomagnetic properties of bismuth was unsatisfactory. Consequently, Abeles and Meiboom[87] carried out thorough experiments on the anisotropy of the Hall effect and magnetoresistance in bismuth in order to develop a more satisfactory model of the band structure. They made measurements on single crystals of pure and tin-doped bismuth as a function of temperature be-

[84] F. J. Morin and J. P. Maita, Phys. Rev. 94, 1525 (1954); 96, 28 (1954).
[85] G. G. Macfarlane and V. Roberts, Phys. Rev. 97, 1714 (1955); 98, 1865 (1955).
[86] Crawford, Schweinler, and Stevens, Phys. Rev. 99, 1330 (1955).
[87] B. Abeles and S. Meiboom, Phys. Rev. 101, 544 (1956).

TABLE III. Low field magnetoresistance calculations in p-type germanium and silicon.

Coefficient $\times 10^9$	Germanium 77°K Obs[a]	Germanium 77°K Calc[b]	Germanium 300°K Obs[a]	Germanium 300°K Calc[c]	Silicon 78°K Obs[d]	Silicon 78°K Calc[f]
$\frac{M_{100}}{H^2}$	0.14	0.093	0.04	0.004	0.5	0.018
$\frac{M_{110}}{H^2}$	2.0	3.25	0.21	0.12	0.5	0.44
$\frac{M_{100}^{010}}{H^2}$	30.4	30.4	1.3	1.3	1.6[e]	1.6
$\frac{M_{110}^{1\bar{1}0}}{H^2}$	27.0	27.4	1.3	1.2		
$\frac{M_{110}^{001}}{H^2}$					2.0	1.6

[a] See reference 67.
[b] Calculated assuming an energy independent $\tau = 1.025 \times 10^{-12}$ for both holes.
[c] Calculated assuming both are lattice scattered and $\bar{\tau}_L = \bar{\tau}_H = 1.51 \times 10^{-13}$.
[d] See reference 70; these results are for $B = 4400$ gauss.
[e] Pearson and Herring give M_{100}^{001}/H^2 which equals M_{100}^{010}/H^2 because of cubic symmetry.
[f] Calculated assuming an energy independent $\tau = 7.7 \times 10^{-13}$ for both holes.

tween 80 and 300°K and as a function of magnetic field up to 2000 gauss. In order to explain their experimental data similar to that shown in Fig. 28, they developed a phenomenological theory which assumed that the valence and conduction bands overlap and also that the energy surfaces near the extrema were ellipsoids. Since the arrangement and number of ellipsoidal surfaces in energy-momentum space must have rhombohedral symmetry, they assumed the following: The holes move on one set of ellipsoids of revolution with the major axis parallel to the trigonal axis of the crystal. The electrons move on three ellipsoidal surfaces having one axis parallel to the trigonal axis and another parallel to the binary axis. The three ellipsoids transform into

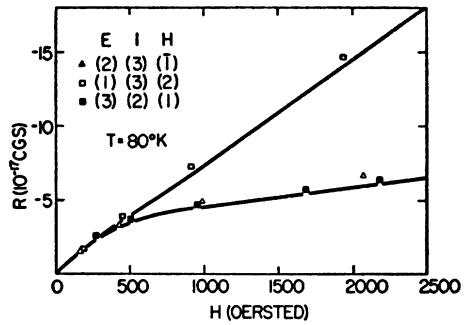

FIG. 28. Hall field in bismuth as function of magnetic field at 80°K. Points indicate experimental values; curves calculated using phenomenological theory and values of parameters given in Table IV. Directions of current **I**, magnetic field **H**, and observed component of electric field **E** are given. (3) denotes the trigonal axis, (1) a binary axis and (2) indicates the direction perpendicular to (1) and (3). (After Abeles and Meiboom.)

TABLE IV. Electron and hole mobilities in Bi, μ, and ν, respectively. Subscripts 1, 2, and 2 refer to the two binary and to the trigonal axes. All quantities are in cgs units. (After Abeles and Meiboom.)

	300°K	80°K
$N, P\times10^{-18}$	2.2	0.46
$\mu_1\times10^{-6}$	9.5	167
$\mu_2\times10^{-6}$	0.24	4.2
$\mu_3\times10^{-6}$	5.7	100
$\nu_1, \nu_2\times10^{-6}$	2.3	37
$\nu_3\times10^{-6}$	0.62	10

one another by a rotation of 120° about the trigonal axis. They also assumed that the relaxation time τ of the electrons and holes is independent of energy. They worked out the phenomenological theory by calculating the conductivity tensors of each ellipsoid in a manner analogous to that described for germanium. They obtained a total conductivity for all ellipsoids and by inversion obtained the relation between electric field and current, and also obtained expressions for the Hall and magnetoconductivity coefficients. They compared the results with experiments obtaining the numerical values for the mobilities in Table IV. These values were used to obtain theoretical curves in reasonably good agreement with experiments as shown by the solid lines of Fig. 28.

The important thing here is that the galvanomagnetic measurements have given a very good qualitative picture of the energy bands in terms of the ellipsoidal model. Unfortunately, however, the quantitative values of the masses or even the mass ratios in this case are unobtainable. However, one can take the mass ratios from the de Haas-van Alphen data for electrons as $m_1:m_2:m_3\approx1:500:10$ (neglecting the slight tilt of 6° of the ellipsoids out of the trigonal plane). Since the galvanomagnetic measurements give results in terms of mobility, or τ/m^*, one can estimate the anisotropy of the scattering using the data of Abeles and Meiboom[87] and obtain $\tau_1:\tau_2:\tau_3\approx1:13:5$. These numbers are approximate, of course, but they do indicate that the scattering is anisotropic and hence one cannot obtain quantitative values of the mass ratios.§

Abeles and Meiboom did not report the longitudinal magnetoresistance along the trigonal axis which indicates that they assumed that the ellipsoids lie in the trigonal plane. Actually, however, the ellipsoids are tilted slightly out of the plane. Since the tilt is small, only 6°, one would expect that the component of motion of the electron along the direction of the magnetic field (oriented in the trigonal direction) would be small and would give rise to only a very small value of longitudinal magnetoresistance. Nevertheless, the presence of this component has been observed by Babiskin.[60] Consequently, one must conclude that the ellipsoidal model for the electrons as predicted by Shoenberg is correct. The single ellipsoid of revolution for the holes in bismuth is essentially the model suggested by Berlincourt[88] for arsenic where he had observed two sets of oscillations in his de Haas-van Alphen data.

§ Recent cyclotron resonance results of Aubrey and Chambers[38] do not agree completely with Shoenberg's effective mass ratios in bismuth. Their results, combined with those of Abeles and Meiboom[87] indicate a much smaller anisotropy of τ.

Other Metals

Much experimental work has been done on the galvanomagnetic properties of metals including single crystal measurements. However, the analytical work on the band structure of these metals has not been carried out to the same degree as it has in germanium, silicon, and bismuth. A good review of the situation is given by Borovik.[89] Following the scheme of Justi[90] he classifies metals in accordance with the behavior of their magnetoresistance at very high fields. Metals such as bismuth, antimony, arsenic, gallium, tungsten, cadmium, beryllium, zinc, lead, tin, carbon, and magnesium belong to the class in which the magnetoresistance steadily increases at high magnetic fields. The magnetoresistance of aluminum, indium, and sodium apparently tends to a limiting value at high magnetic fields. In addition, Borovik classified his metals in accordance with the behavior of the tangent of the Hall angle, $\tan\theta=E_y/E_x$, where E_y is the Hall voltage and E_x is the applied longitudinal voltage. In the metals of the first class $|E_y/E_x|$ increases to a maximum, then falls off at high fields. In the second class which includes aluminum, indium, copper, and sodium $|E_y/E_x|$ increases indefinitely with magnetic field. These properties represent average effects in a transverse magnetic field. The single crystal behavior conforms to this

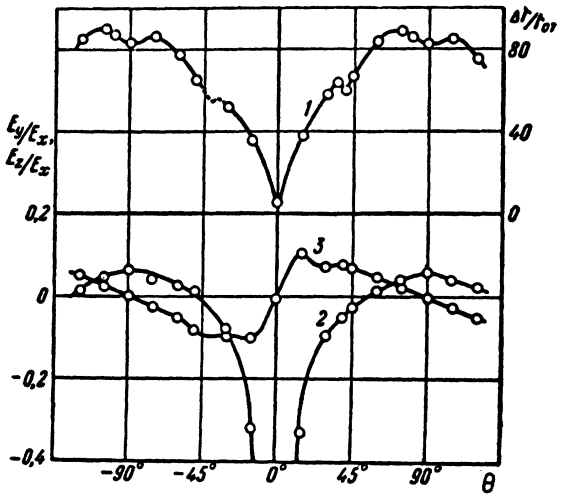

FIG. 29. Hall effect and change in resistance in tin. $T=4.22$°K; $H=14\,880$ oersteds. Curve 1: Magnetoresistance $\Delta\rho/\rho_0$; 2: E_y/E_x; 3: E_z/E_x; θ: angle between fourth-order symmetry axis and magnetic field. At $\theta=0°$, $E_y/E_x=-2.46$. (After Borovik.)

[88] T. G. Berlincourt, Phys. Rev. **99**, 1716 (1955).
[89] E. S. Borovik, Bull. Acad. Sci. USSR **19**, 429 (1955).
[90] E. Justi, Physik Z. **41**, 563 (1940); Leitfähigkeit and Leitungsmechanismus fester Stoffe, Göttingen (1948).

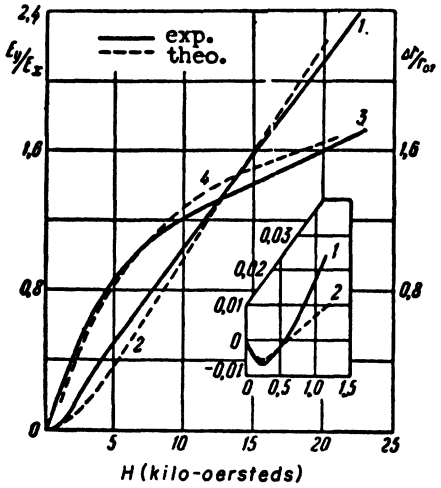

FIG. 30. Comparison of experimental and calculated values of Hall field and change in resistance in magnetic fields for aluminum. $T=4.22°K$. Curves 1 and 2: E_y/E_x; curves 3 and 4: $\Delta\rho/\rho_0$. (After Borovik.)

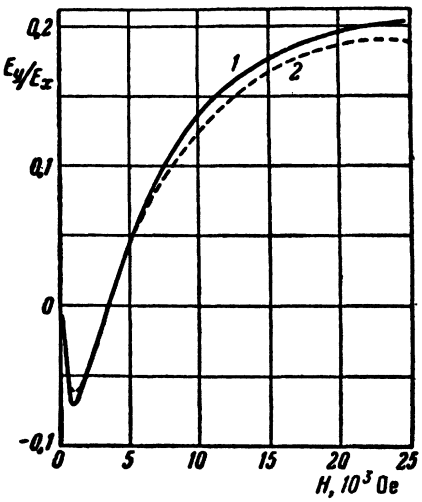

FIG. 31. Comparison of experimental (1) and theoretical (2) values of Hall field for magnesium at 4.22°K. (After Borovik.)

general picture, but the over-all behavior at low and intermediate fields shows effects which depend on the orientation of the crystal. Such anisotropy effects were obtained by Borovik for tin (Fig. 29) and zinc for both the magnetoresistance and the Hall effect. These two metals show very marked anisotropy in the presence of a magnetic field. Such anisotropy with corresponding magnetoresistance minima has been observed[91] in gallium, zinc, cadmium, and gold. Anisotropy in these materials is significant in that it gives some information on the characteristics of the energy surfaces. For cubic crystals, one might be led to expect spherical energy surfaces because symmetry requires that the normal resistance be isotropic. Nevertheless, in these metallic crystals with cubic symmetry, the longitudinal magnetoresistance in some directions is not zero and the transverse magnetoresistance depends on the orientation of the magnetic field relative to the axes, indicating very anisotropic surfaces. This anisotropy effect in a material like gold is quite pronounced. Unfortunately, no quantitative theoretical analysis of these anisotropy effects has been made. However, as in the case of germanium, silicon, and bismuth, these effects are associated with the anisotropic energy surfaces of these metals. Presumably the properties of the energy surfaces of the metals will soon be determined by methods that will make use of data of this sort.

Detailed knowledge of the nature of the energy surfaces in these materials is lacking so that, in order to analyze the data, it has been necessary to assume a model of two isotropic carriers. For this model

$$\frac{E_y}{E_x}=\frac{n_1\phi_1^2/(1+\phi_1^2)-n_2\phi_2^2/(1+\phi_2^2)}{n_1\phi_1/(1+\phi_1^2)+n_2\phi_2/(1+\phi_2^2)}, \tag{22}$$

[91] W. de Haas and J. Blom, Physica **1**, 134 (1934); Lazarev, Nakhimovich, and Parfenova, Zhur. Eksptl. i Teoret. Fiz. **9**, 1169 (1939); E. Justi and H. Scheffers, Physik Z. **37**, 475 (1936); Justi, Kramer, and Schultze, Physik Z. **41**, 308 (1940).

and the magnetoconductivity is given by

$$\sigma_H=\left(\frac{\sigma_{01}}{1+\phi_1^2}+\frac{\sigma_{02}}{1+\phi_2^2}\right)\left[1+\left(\frac{E_y}{E_x}\right)^2\right], \tag{23}$$

where the subscripts 1 and 2 refer to the two carriers. n_1 is the number of carriers of mass m_1 and mean scattering time τ_1. The zero-field conductivity $\sigma_{01}=n_1e^2\tau_1/m_1$ and $\phi_1=eH\tau_1/m_1c$. The behavior of these quantities at high magnetic fields is different for $n_1=n_2$ than it is for $n_1\neq n_2$. E_y/E_x varies as $1/H$ and that $\Delta\rho/\rho_0$ varies as H^2 for equal numbers of the two carriers. For unequal numbers, E_y/E_x varies as H and $\Delta\rho/\rho_0$ tends to approach a limit at high fields. Thus, qualitatively, the properties of the two types of metals can be classified, the first group consisting of those having equal numbers of holes and electrons, and the second group, unequal numbers of holes and electrons. A typical comparison of theory and experiment for aluminum is shown in Fig. 30 for which $n_1\neq n_2$. The theory describes the behavior fairly well for almost the entire range of magnetic field for the second group. However, for metals in which the number of holes and electrons are equal the agreement is satisfactory for high magnetic fields, but in the low and intermediate field region the theory is not fully satisfactory. Magnesium is one of these metals in which the Hall parameter E_y/E_x first becomes negative at low fields (Fig. 31) and then becomes positive. To explain this, it is necessary to assume that there are two kinds of holes and two kinds of electrons. The theory may be modified accordingly to specify one set of holes having concentration n_1 and n_2 and one set of electrons, n_3 and n_4. Good agreement is obtained when $n_1=n_3$ and $n_2=n_4$ or when $n_1+n_2=n_3+n_4$. The theoretical equations are similar to Eqs. (22) and (23). The assumption of two sets of electrons and holes with different mobilities appears to be necessary for some of the metals

with hexagonal symmetry. Cyclotron resonance data indicate that this is the situation for graphite. In order to explain the behavior of the galvanomagnetic properties of graphite, Soule[92] and McClure[93] have postulated the existence of light and heavy holes and light and heavy electrons. Borovik also indicates that two groups of electrons and holes should be considered for cadmium and zinc.

The galvanomagnetic properties of many other single crystal semiconductors have been and are being investigated. In particular the anisotropy properties of the PbS, PbTe, and PbSe by Allgaier[94] and also by Irie[95] indicate that analysis is forthcoming in the near future which may shed light on the detailed nature of the bands in these materials. In addition, a great deal of work has been carried out on 3–4 and 5–6 compounds in which the Hall measurements have given values for the mobilities of holes and electrons. These measurements do not provide information which could lead to analysis of anisotropy or band structure. Recent careful measurements of the galvanomagnetic properties of InSb have been made by Frederikse and Hosler.[53] They looked for anisotropy of both holes and electrons and apparently found no appreciable effects.

INFRARED ABSORPTION

Prior to the most recent developments, infrared absorption measurements have been used primarily for measuring the energy gap in semiconductors. Free carrier absorption was studied in some of the experiments and the results used to estimate the effective mass. Following the cyclotron resonance work, the infrared absorption experiments have been used to provide information on band structure. Macfarlane and Roberts[85] worked on the interpretation of the infrared absorption at the band edge as related to the detailed structure of germanium and silicon. The interband absorption in p-type germanium observed by Briggs and Fletcher[96] and by Kaiser, Collins, and Fan[97] was interpreted by Kahn[98] using the results of the cyclotron resonance experiments. The anomalous optical absorption in indium antimonide observed by Tanenbaum and Briggs[99] was used by Burstein[100] to estimate the effective mass of electrons and holes in this material. The most significant infrared experiments are those performed recently on the oscillatory magnetoabsorption effect.

Indirect Absorption Edge in Ge and Si

Hall, Bardeen, and Blatt[101] showed theoretically that optical absorption by valence electrons involves two types of transitions called direct and indirect. The direct transition involves the absorption of a photon in which the energy exchange results in the conservation of momentum, or $\Delta k=0$ for the electron. This happens at the center of the Brillouin zone. The indirect transition involves a three body process: phonon, photon, and electron. The electron transition is from the valence band, at the center of the Brillouin zone, to the bottom of the conduction band which is near the edge of the Brillouin zone. The process also involves either the emission or absorption of a phonon. Macfarlane and Roberts set out to test this theory quantitatively and, using the theoretical results of Hall, Bardeen, and Blatt obtain an expression for the absorption coefficient K of the following form

$$K=A\left[\frac{1}{1-e^{-\theta/T}}\left(\frac{h\nu-\epsilon_g-k\theta}{h\nu}\right)^2+\frac{1}{e^{\theta/T}-1}\left(\frac{h\nu-\epsilon_g+k\theta}{h\nu}\right)^2\right], \quad (24)$$

where ϵ_g represents the energy gap and $k\theta$, the energy of a phonon. They carried out careful experiments in both Ge and Si and obtained the values of the absorption coefficient. Then they compared the data with theoretical plots of $K^{\frac{1}{2}}$ for different temperatures (shown in Fig. 32) and showed that one set of straight lines correspond to $\epsilon_g-k\theta<h\nu<\epsilon_g+k\theta$ and a steeper set of straight lines correspond to $h\nu>\epsilon_g+k\theta$. These correspond to the absorption and emission of a phonon involved in the indirect transitions. Thus the first term in Eq. (24) corresponds to a photon absorption with the emission of a phonon of energy $k\theta$ and the second term corresponds to absorption of a phonon of energy $k\theta$. A similar plot was also obtained for silicon by Macfarlane and Roberts.[85] By estimating the value of $\theta=260°$K for Ge and $\theta=600°$K for Si, they obtained a good fit (Fig. 32) to the experimental data for Ge and similarly for Si. They attempted to estimate the position

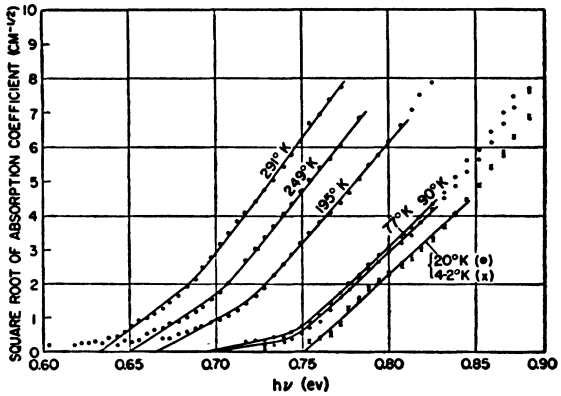

FIG. 32. Dependence of absorption constant on photon energy for 60 ohm cm germanium. Points are experimental and solid lines were calculated from Eq. (24). (After Macfarlane and Roberts.)

[92] D. E. Soule, Bull. Am. Phys. Soc. Ser. II, 1, 255 (1956).
[93] J. W. McClure, Bull. Am. Phys. Soc. Ser. II, 1, 255 (1956).
[94] R. S. Allgaier, Bull. Am. Phys. Soc. Ser. II, 2, 141 (1957).
[95] T. Irie, J. Phys. Soc. Japan 11, 840 (1956).
[96] H. B. Briggs and R. C. Fletcher, Phys. Rev. 91, 1342 (1953).
[97] Kaiser, Collins, and Fan, Phys. Rev. 91, 1380 (1953).
[98] A. H. Kahn, Phys. Rev. 97, 1647 (1955).
[99] M. Tannenbaum and H. B. Briggs, Phys. Rev. 91, 1561 (1953).
[100] E. Burstein, Phys. Rev. 93, 632 (1954).
[101] Hall, Bardeen, and Blatt, Phys. Rev. 95, 559 (1954).

of the conduction band minima in momentum space by using cyclotron resonance data, elastic constants, and the theory of vibrations of the diamond lattice. In germanium, they estimated that the minimum occurred at about $\frac{2}{3}$ of the distance from the center to the edge of the Brillouin zone using a [111] direction. This was not quite correct because it is now known that the minima are at the edge of the zone.[69,86] In silicon they estimated the position of the minimum to be 7/9 of the distance from the center of the zone along the [100] direction. This quantitative value of the position may be approximate for Si but it is consistent with the theory[102] that the minima are neither at the center nor at the edge. Macfarlane and Roberts also evaluated (Fig. 27) the temperature dependence of the energy gap for both materials. Fan, Shepard, and Spitzer[103] discussed the application of the HBB theory to the infrared absorption in Ge and Si and have shown that the results of the optical, electrical, and cyclotron resonance measurements are consistent with the band structure of these materials.

In the study of the band structure of semiconductors, several ingenious techniques have been used for examining the relative motion of the bands. Paul and Brooks[104] and also Herman[105] have predicted that a sufficiently high pressure would enable one to interchange [111] and [100] minima in Ge as the bottom of the conduction band. Warschauer, Paul, and Brooks[106] and Spitzer, Bennett, and Fan[107] have used infrared absorption in Ge to examine the shift of the absorption edge with pressure. Another useful scheme for studying the shift of the band minima as a function of the crystal parameters has been the examination of the properties of Ge-Si alloys. Johnson and Christian[108] and Levitas, Wang, and Alexander[109] have measured the variation in the energy gap as a function of alloying content and showed a sharp break at 15% silicon. Herman[110] has interpreted the behavior of the band minima as follows: up to 15 mole percent silicon, the band minimum is along the [111] direction as in germanium whereas, above this value, the band minimum occurs along the [100] direction. Further confirmation of the interchange of these minima was given by Paul and Warschauer[111] who studied the infrared absorption of a number of Ge-Si alloys under high pressure.

[102] W. Kohn, Phys. Rev. **98**, 1561 (1955).
[103] Fan, Shepard, and Spitzer, *Proceedings of the Atlantic City Photoconductivity Conference, 1954* (John Wiley and Sons, Inc., New York, 1955).
[104] W. Paul and H. Brooks, Phys. Rev. **94**, 1128 (1954).
[105] F. Herman, Physica **20**, 801 (1954).
[106] Warschauer, Paul, and Brooks, Phys. Rev. **98**, 1193 (1955).
[107] Spitzer, Bennett, and Fan, Phys. Rev. **98**, 288 (1955).
[108] E. R. Johnson and S. M. Christian, Phys. Rev. **95**, 560 (1954).
[109] Levitas, Wang, and Alexander, Phys. Rev. **95**, 846 (1954).
[110] F. Herman, Phys. Rev. **95**, 847 (1954).
[111] W. Paul and D. M. Warschauer, Bull. Am. Phys. Soc. Ser. II, **1**, 266 (1956).

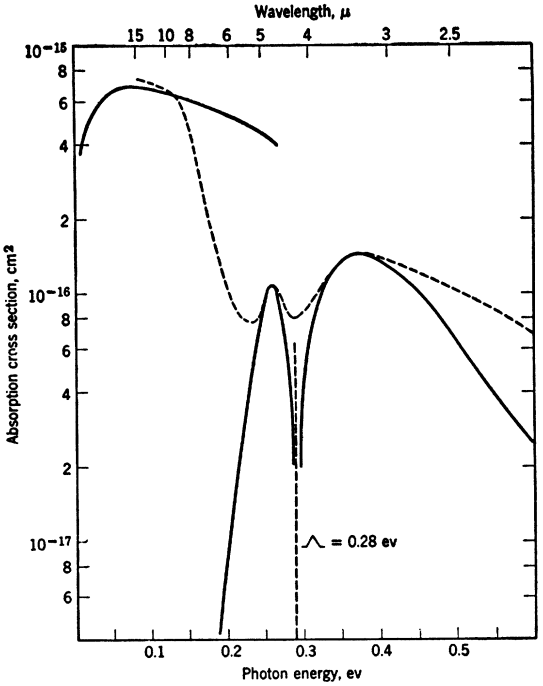

FIG. 33. Absorption cross section of free-charge carriers in *p*-type germanium. Dashed line: room-temperature data of Briggs and Fletcher. Solid line: calculations of Teitler, Burstein, and Lax (unpublished) and A. H. Kahn. (After Burstein, Picus, and Sclar.)

Direct Transition

In order to confirm the theoretical prediction of the direct transitions in Ge and Si, Dash and Newman[112] carried out absorption experiments in high purity single crystals at 77°K and 300°K. They used very thin samples (a few microns) measured accurately by the interference fringe patterns in the infrared transmission. The results showed two distinct steep portions in the absorption curve corresponding to the indirect and direct transitions. They interpret their data for germanium to have direct transitions at 0.81 ev at 300°K and 0.88 ev at 77°K. For the indirect transitions, which correspond to the gap, they obtained 0.62 ev at 300°K and 0.72 ev at 77°K. In silicon, they estimated the direct transition from the 77° data to be about 2.5 ev. For the indirect (energy gap) transition, they obtained 1.06 ev and 1.16 ev at 300° and 77°K, respectively.

Interband Transitions in *p*-Type Germanium

Experimental observation of absorption in *p*-type germanium[113] has shown absorption maxima (Fig. 33) from 2 to 30 microns. This effect was first reported by Briggs and Fletcher and also by Kaiser, Collins, and Fan.[97] The former, in a subsequent publication[96] interpreted this phenomenon in terms of interband transitions between three valence bands in Ge. Although

[112] W. C. Dash and R. Newman, Phys. Rev. **99**, 1151 (1955).
[113] H. B. Briggs and R. C. Fletcher, Phys. Rev. **87**, 1130 (1952).

qualitatively this mechanism was correct, the quantitative interpretation given by Kahn[98] utilized the data of the microwave cyclotron resonance experiments. The graph of Fig. 33 shows the experimental data and the theoretical curves of Kahn which were also calculated by Teitler, Burstein, and M. Lax.[114] Kahn showed that the two absorption peaks at photon energies of about 0.25 ev and about 0.4 ev correspond to the transitions between the split-off Γ_{25} band and the upper two degenerate bands. The long wavelength absorption peak at about 0.08 ev corresponds to transitions between the two upper degenerate bands.

Absorption in InSb

Tanenbaum and Briggs[99] discovered that the optical absorption at the band edge has an anomalous dependence on the impurity concentration in InSb. They discovered that the apparent energy gap increases from about 7 μ for a pure sample to 3 μ for one that contained n-type impurities of about 5×10^{18} electrons per cubic centimeter. This effect was first explained by Burstein[100] and independently by Moss[115] on the basis of the high curvature of the conduction band in InSb. Because of the existence of a small effective mass, m_e, for the electron, the density of states (proportional to $m_e^{\frac{3}{2}}$) is relatively small. Consequently the excess electrons from the impurities fill up the states fairly rapidly with increasing concentration. InSb becomes degenerate at relatively low electron densities and the height of the Fermi level also rises with impurity concentration. The optical transition, which takes place from the top of the valence band to levels a few kT below the Fermi level in the conduction band, consequently increases in energy with concentration. Using this as a basis and the expression for the density of states for a band with spherical energy surfaces, Burstein and also Moss were able to evaluate the effective mass of the electrons from the relation

$$m_e/m_0=4\times10^{-15}N^{\frac{2}{3}}\Delta\epsilon^{-1},$$

where N is the total number of states in an energy interval $\Delta\epsilon$ above the bottom of the conduction band. Estimating a shift of 0.019 ev for the absorption edge corresponding to 1.5×10^{18} carriers per cubic centimeter, one obtains a value of $m_e\approx0.03m_0$. Using the value of Tanenbaum and Maita[116] of the product, $(m_em_h)^{\frac{1}{2}}=0.083m_0$ obtained from Hall constant and conductivity measurements, the mass of the hole was estimated to be $m_h\approx0.2m_0$. Moss also obtained an independent estimate of the mass from the free carrier absorption of infrared radiation at longer wavelengths using the Drude-Zener theory, and also from analysis of the variation of the absorption edge with temperature. This gave good agreement with estimates from impurity studies.

Hrostowski, Wheatley, and Flood[117] made a comparison between the simple theory and the experiment in InSb of the anomalous absorption as a function of impurity concentration. They conclude that the energy band is not parabolic over the range that they analyzed. More refined calculations by Kaiser and Fan[118] and also by Stern and Talley[119] of the shift of the Fermi level with impurity concentration confirms the general picture in InSb. The comparison of the theory and experiment is indicated in Fig. 34. Stern and Talley also applied their theory to analysis of anomalous absorption in InAs and found for the electron mass, $m_e\approx0.055m_0$. The electron masses obtained are approximately twice the value of those obtained from microwave and infrared cyclotron resonance at low magnetic fields. The infrared cyclotron resonance experiments[38] with pulsed magnetic fields have resolved this discrepancy, since they demonstrated that curvature of the energy band is nonparabolic, and that it decreases with increasing energy. This general picture was consistent with the results of Fan[120] who estimated the effective masses in InSb as a function of impurity concentration using the Drude-Zener theory for free carrier absorption. He also obtained a value of the effective mass for InAs, $m_e=0.03m_0$, from free carrier absorption measurements, in good agreement with results from infrared cyclotron resonance. Independent studies by Barrie and Edmond[121] of the conduction band in InSb using doped material up to 10^{19} carriers/cm^3 and analyzing the measurements of the optical gap, thermoelectric power, the Hall constant and the conductivity, result in agreement with Hrostowski *et al.*[117] of the nonparabolic nature of the conduction band. They found from the optical data that $m_e=0.03m_0$, but from the thermoelectric power and mobility data that $m_e\approx0.02m_0$. Frederikse

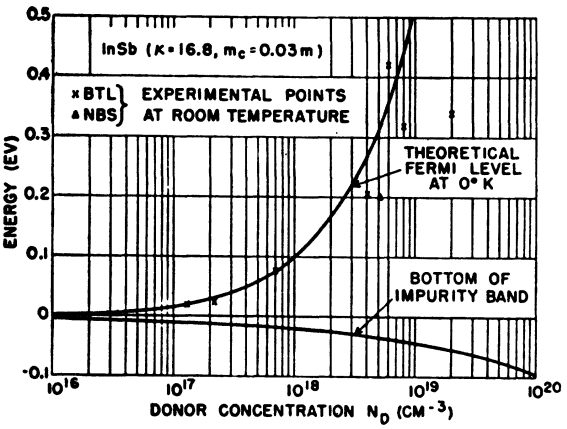

FIG. 34. Comparison of theory and experiment for InSb. Curves are theoretical. κ is the dielectric constant and m_c is effective mass of electron. Points marked BTL and NBS are experimental results. (After Stern and Talley.)

[114] Burstein, Picus, and Sclar, see reference 103.
[115] T. S. Moss, see reference 103.
[116] M. Tannenbaum and J. P. Maita, Phys. Rev. **91**, 1009 (1953).
[117] Hrostowski, Wheatley, and Flood, Phys. Rev. **95**, 1683 (1954).
[118] W. Kaiser and H. Y. Fan, Phys. Rev. **98**, 966 (1955).
[119] F. Stern and R. M. Talley, Phys. Rev. **100**, 1638 (1955).
[120] W. Spitzer and H. Y. Fan, Phys. Rev. **106**, 882 (1957).
[121] R. Barrie and J. T. Edmond, J. Electronics **1**, 161 (1955).

and Mielczarek[122] conclude from their thermoelectric power measurements on InSb between 160°K and 200°K that the effective mass of the electron is $0.014m_0$. They combine this with their measured mass ratios and deduce an effective mass of the hole of $0.13m_0$. Hrostowski and co-workers[123] also found that a lower value of the effective mass, $m_e=0.015m_0$, gave the best fit to their electron mobility data. Chasmar and Stratton[124] gave further verification of the variation of effective mass with energy from their Hall coefficient and thermoelectric measurements giving effective mass values for electrons in InSb and InAs as a function of kT which represented the average energy of the electrons. Their data for InSb appear to be in close agreement with that obtained from the infrared cyclotron resonance measurements.

Although these measurements permit an estimate of the effective mass of hole in InSb, the nature of the valence band was obscured. However, Roberts and Quarrington[125] conclude, in their study of absorption in InSb and GaSb, that indirect transitions are effective in these materials and that, consequently, the minimum of the conduction band or the maximum of the valence band were not at the center of the Brillouin zone. Subsequent detailed analysis of the absorption edge in InSb by Blount and co-workers[126] indicates the existence of two bands that give rise to two indirect transitions. They estimate that the two valence bands involved have an energy separation of about 0.025 ev. These conclusions appear to contradict the results of the oscillatory magnetoabsorption effect in InSb.

Oscillatory Magnetoabsorption Effect

The first evidence of the oscillatory magnetoabsorption effect appeared in a study by the Lincoln group[127] of the direct transition in germanium. A detailed account was subsequently given by Zwerdling and Lax.[128] This phenomenon was independently observed by Burstein and Picus[129] in InSb. Subsequently Lax, Zwerdling, and Roth[130] investigated this effect in both InSb and InAs. The important anisotropy of the oscillatory magnetoabsorption effect which is interlinked with the detailed nature of the band structure in these semiconductors was observed by the Lincoln group.[128,131]

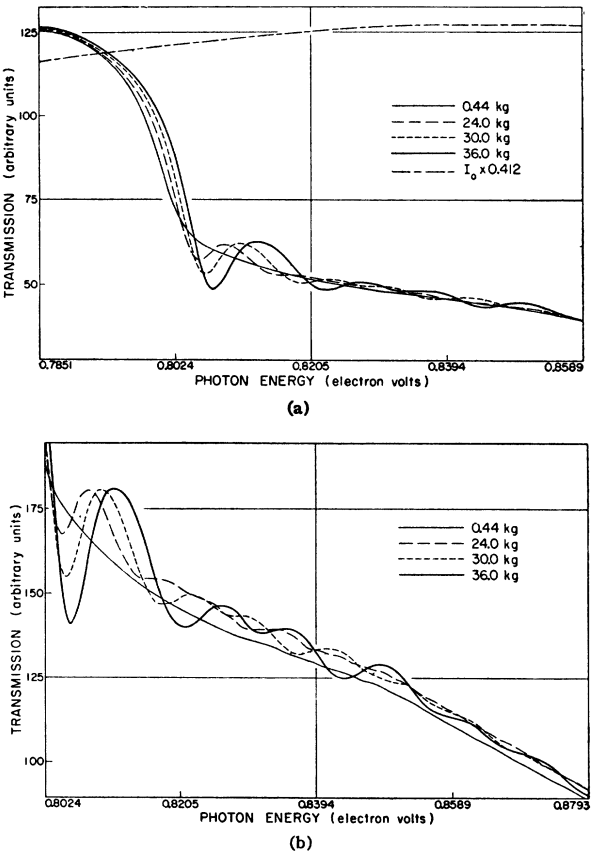

FIG. 35. (a) Absorption edge and oscillatory magnetoabsorption for direct transition in germanium. (b) Magnified traces of transmission minima and maxima at photon energies above the absorption edge. (After Zwerdling and Lax.)

The latter have given[132] a quantitative theoretical interpretation of the spectrum and the anisotropy in germanium.

Germanium

The oscillatory magnetoabsorption effect in Ge has been observed at room temperature, 77°K and 4°K at infrared wavelengths corresponding to the direct transition[112] in Ge in the presence of a magnetic field. The measurements have been carried out on two sets of single crystals approximately 4 and 7 μ thick. The magnetic field, was applied in a direction parallel to the sample surface. Several fixed values were chosen up to a maximum 36 000 gauss and the infrared wavelength was scanned through the suitable range near the direct transition absorption edge. The results for these experiments are shown in Figs. 35 and 36. The existence of the transmission minima are interpreted as transitions from the Landau levels of the Γ_{25}^+ valence bands to the Γ_2^- conduction band. The transitions corresponding to these minima are shown schematically in Fig. 37. The

[122] H. P. R. Frederikse and E. V. Mielczarek, Phys. Rev. **99**, 1889 (1955).
[123] Hrostowski, Morin, Geballe, and Wheatley, Phys. Rev. **100**, 1672 (1955).
[124] R. P. Chasmar and R. Stratton, Phys. Rev. **102**, 1686 (1956).
[125] V. Roberts and J. E. Quarrington, J. Electronics **1**, 152 (1955).
[126] Blount, Callaway, Cohen, Dumke, and Phillips, Phys. Rev. **101**, 563 (1956).
[127] Zwerdling, Keyes, Foner, Kolm, and Lax, Phys. Rev. **104**, 1805 (1956).
[128] S. Zwerdling and B. Lax, Phys. Rev. **106**, 51 (1957).
[129] E. Burstein and G. S. Picus, Phys. Rev. **105**, 1123 (1957).
[130] Lax, Zwerdling, and Roth, Bull. Am. Phys. Soc. Ser. II, **2**, 141 (1957).
[131] S. Zwerdling and B. Lax, Bull. Am. Phys. Soc. Ser. II, **2**, 141 (1957).
[132] Roth, Lax, and Zwerdling, Bull. Am. Phys. Soc. Ser. II, **2**, 141 (1957).

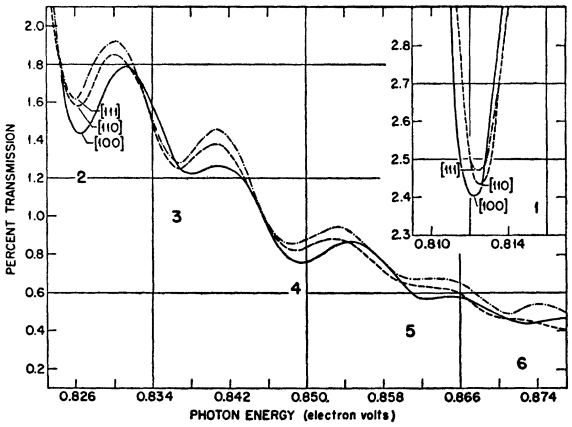

FIG. 36. Anisotropy of oscillatory magnetoabsorption in germanium showing change in amplitude and shift in transmission minima and maxima for magnetic field along three principal crystal directions. Inset shows a magnified trace of the first minimum. (After Zwerdling and Lax.)

selection rules have been worked out theoretically[132] and show that the transitions between the Landau levels of the two sets of bands require that $\Delta n=0$ and $\Delta n=-2$ between the appropriate magnetic levels. The calculations of the energy spectrum for the line structure associated with these transitions has used the results of Luttinger and Kohn[133] as modified by Luttinger.[134] As shown in Fig. 38, the correlation between the experimental results and the weighted mean of the fine structure is reasonably good. The theoretical results also account semiquantitatively for the anisotropy of the effect in germanium as shown in Table V. A discrepancy in sign of the anisotropy shift of the first minimum indicates the necessity of further extension of the theory. One obvious extension for evaluating of the spectral lines is to include all values of the momentum component along the direction of the magnetic field. This is rather difficult to do.

Figure 39 shows a plot of the positions of the consecutive minima in terms of photon energy as a function of magnetic field. The figure shows a series of straight lines through the experimental points, converging to a single point at $B=0$. The significance of these curves is that the bands are quadratic in k for the range of B up to 36 000 gauss and that all the Landau levels which are linear in B collapse to the bottom of the band at $B=0$. This appears to be an accurate method for measuring the gap spacing at $k=0$ and gives a value of 0.803 $\pm$0.001 ev at room temperature. The change in the gap energy at $k=0$ with magnetic field is given by $\Delta\epsilon=1/2\hbar(\omega_{c1}+\omega_{c2})$ where ω_{c1} is the cyclotron frequency for the conduction band and ω_{c2} that for the valence band at $k=0$. We assume that for the latter the Landau level for $n=0$ corresponds approximately to that of the large hole mass, $m_v\approx 0.33m_0$. This leads to $1/m^*=1/m_c+1/m_v$, where $m^*\approx(0.038\pm 0.003)m_0$ is the mass determined from the slope of magneto-gap shift. Since

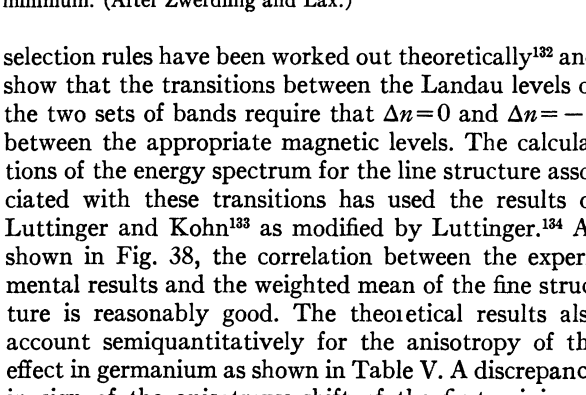

FIG. 37. A schematic diagram of the transitions between magnetic levels of the valence and conduction bands in germanium. (After Roth, Lax, and Zwerdling.)

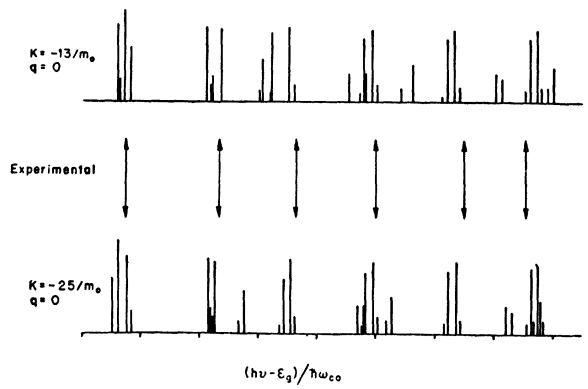

FIG. 38. Correlation between experiment and theory of the oscillatory magneto-absorption in germanium. Detailed upper and lower spectrum are result of theoretical calculations of absorption for two different values of the constant K. $K=13/m_0$ is that suggested by Luttinger and $K=-25/m_0$ was used by Roth, Lax, and Zwerdling. (After Roth, Lax, and Zwerdling.)

$m_v\gg m^*$, $m_c\approx m^*(1+m^*/m_v)\approx 0.042m_0$. Another estimate of effective mass of the electrons can be made by using the diagram of Fig. 37. The difference between higher quantum transitions corresponding to the differences between lines 5 and 6 and lines 6 and 7 in Fig. 39 can be represented approximately by the difference between two adjacent large mass Landau levels and two adjacent electron levels of the same quantum numbers respectively. Consequently, $\Delta\epsilon=\hbar(\omega_{c1}+\omega_{c2})\approx 0.0097$ ev at 30 000 gauss. Using similar corrections as before, one obtains $m_c^*\approx 0.039m_0$. These values are in good agreement with the theoretical estimate of $\sim 0.034m_0$ by Dresselhaus, Kip, and Kittel[17] from cyclotron resonance data. Another theoretical estimate of the conduction band electron effective mass at $k=0$ has been published by Dumke.[135] He finds $m_c^*\sim 0.037m_0$. The results at 77°K and 4°K give values of the energy gap for the direct transition which are 0.890$\pm$0.002 ev and 0.896

[133] J. M. Luttinger and W. Kohn, Phys. Rev. **97**, 869 (1955).
[134] J. M. Luttinger, Phys. Rev. **102**, 1030 (1956).
[135] W. P. Dumke, Phys. Rev. **105**, 139 (1957).

± 0.002 ev, respectively. The estimate of the effective mass m_c^* indicates no change within experimental error.

Indium Antimonide

In the experiments on the oscillatory magnetoabsorption in InSb, the samples were mounted on thin wafers of Ge or Si with Allymer cement and polished down to thicknesses of ~ 10 to 15 μ. The transmitted infrared radiation through the samples over a wavelength range of 5 to 7 μ showed the characteristic atmospheric absorption bands. These measurements were carried out for different values of the magnetic field. Since the object of the experiment was to compare the transmission properties with and without a magnetic field, the ratios of the intensity of the transmitted signal $I_t(B)/I_t(0)$ automatically eliminate the atmospheric absorption bands because

$$I_t(B)/I_t(0) = \exp[-(\alpha_B - \alpha_0)\delta], \qquad (25)$$

where α_B is the absorption coefficient with magnetic field and α_0, at zero field. δ is the thickness of the sample. In Eq. (25) it is tacitly assumed that the reflection coefficient is not seriously affected by the magnetic field. Furthermore, the graphical plot of this ratio should give the location of the minima as a function of photon energy corresponding to the minima of the differential absorption coefficient, $\Delta\alpha$.

TABLE V. Anisotropy of the oscillatory magnetoabsorption in germanium: $(h\nu_{[111]} - h\nu_{[100]})/h\nu_{c0}$.

Line	Calculated	Observed
1	−0.6	+0.5
2	−1.0	−1.0
3	−3.9	−5.3
4	−1.7	−2.4

The results plotted in this way (Fig. 40) demonstrate the oscillatory magnetoabsorption effect similar to that in germanium. The anisotropy of the transmission minima for different orientations of the magnetic field is not very large: ~ 0.0005 ev at 36.9 kilogauss for the first minimum, negligible for the second minimum, and was not yet studied for the succeeding minima. Plotting the positions of the minima in terms of photon energy as a function of magnetic field, the straight lines associated with the different transitions extrapolate (Fig. 41) to the same value of energy, 0.180 ± 0.002 ev, at zero magnetic field. This implies that the transitions occur at $k=0$ from a common set of valence bands to the conduction band.

A proposed band structure for InSb has been given by E. O. Kane[136] from perturbation theory that suggests a light hole band whose mass is $\sim 0.015 m_0$ and a heavy hole band whose maximum may be displaced slightly from $k=0$. Tentative interpretation of the transitions

[136] E. O. Kane, J. Phys. Chem. Solids 1, 249 (1957).

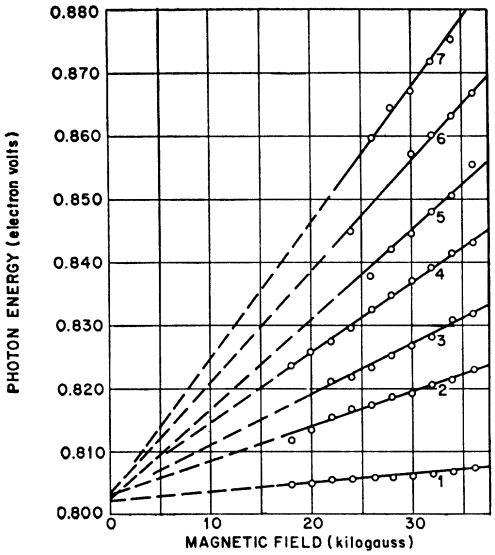

FIG. 39. A plot of transmission minima for germanium in terms of photon energy as a function of magnetic field. The energy 0.803 ± 0.001 ev at $H=0$ is the gap for the direct transition. (After Zwerdling and Lax.)

and related selection rules in InSb have been given by Burstein and Picus[129]; however, not all of the experimental results of the Lincoln and NRL groups are fully consistent with this interpretation. It appears that a detailed theory of the magnetic level structure similar to that developed for Ge is necessary before one can make a satisfactory interpretation of the oscillatory spectrum.

Indium Arsenide

Similar experiments were also carried out on InAs on samples which were ~ 15 μ thick and mounted on Ge.

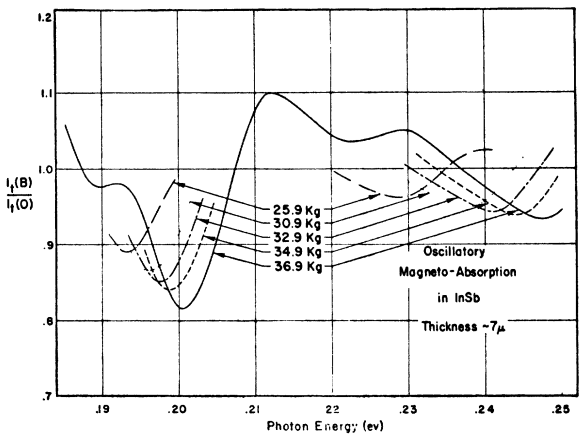

FIG. 40. Representative trace of the ratio of the transmission signals with and without magnetic field as a function of photon energy for a 7-μ single crystal sample of InSb. Magnetic field along [110] direction. For simplicity of presentation only the two prominent minima were drawn for fields below 36.9 kilogauss. (After Lax, Zwerdling, and Roth.)

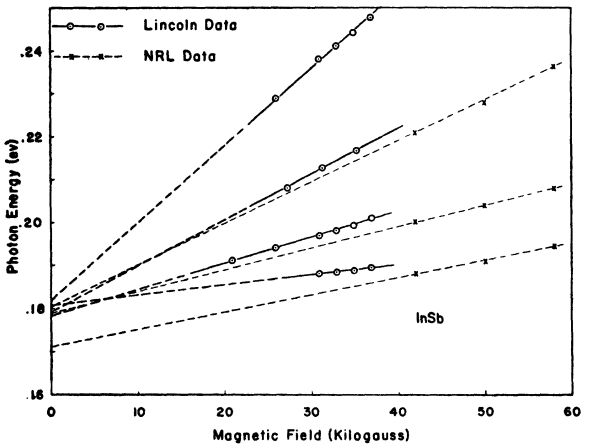

FIG. 41. A plot of position of transmission minima for InSb in terms of photon energy as a function of magnetic field. The heavy lines represent reproducible data for several single crystal samples from 7 to 15 μ thick. The NRL data were taken from data published by Burstein and Picus. The extrapolated value obtained for the energy gap from the Lincoln data is 0.180 ± 0.002 ev. (After Lax, Zwerdling, and Roth.)

These were polycrystalline material, n-type, with 10^{16} to 10^{17} carriers per cubic centimeter. The oscillatory effect was definitely observed, but the amplitude was smaller than that observed in Ge or InSb. However, although the ratio $I_t(B)/I_t(0)$ was close to unity, the first and second minima were detected at high fields. From the slope of the $\Delta\epsilon$ *vs* B curve of the first minimum, an effective mass of the electron was estimated to be $\sim 0.03m_0$ assuming that the mass of the hole was relatively large. The extrapolated value of the energy gap was 0.360 ± 0.002 ev.

From the oscillatory magnetoabsorption measurements at room temperature in germanium, InSb, and InAs, it was evident that the position of the energy gap was at the foot of the transmission curve or the top of the absorption edge. This indicated unequivocally that transitions near $k=0$ occurred for photon energies below that of the energy gap. The only conclusion is that the additional energy which for these materials at room temperature is of the order of 0.02 ev was derived from a phonon. Independently, on theoretical grounds, Dumke came to this same conclusion and suggested that an optical phonon was involved. This obviates the necessity of invoking an indirect transition to account for the energy dependence of the absorption coefficient which does not obey the $(\epsilon-\epsilon_0)^{\frac{1}{2}}$ relation. The hypothesis of a band slightly displaced from $k=0$ at a higher energy would result in the convergence of the various Landau levels to two separate energy gaps separated by the estimated 0.025 ev.[126] The absorption edge and the oscillatory components in InSb and InAs behave remarkably like those in germanium showing very similar structure. This leads one to believe that the valence bands and conduction bands at $k=0$ are perhaps similar and the former are perhaps degenerate.

In order to obtain quantitative correlation with the theory of the spectrum for the oscillatory magnetoabsorption, it will be necessary to go to lower temperatures or high magnetic fields or both in order to resolve the fine structure predicted by Roth *et al.*[132] This would have the advantage of sharpening the lines and perhaps increasing the amplitude, thus improving the resolution.

CONCLUSION

This review of the experimental studies of energy band structure in semiconductors and metals has been somewhat restricted. The author has limited himself to the selection of the material that is most familiar to him which illustrates some of the principal techniques and results under the four major topics. Undoubtedly, much excellent work has been omitted. In particular, a detailed discussion of the large body of literature of the galvanomagnetic effects and the oscillatory phenomena associated with it has been left out. The pioneering work of C. S. Smith[137] in applying piezoresistance measurements for interpreting band structure in Ge and Si has also been omitted. The discussion and possible usefulness of the steady component of the magnetic susceptibility was also not treated. The emphasis has been placed upon more recent investigations.

In concluding, certain remarks about possibilities for the future may be made. The cyclotron resonance phenomenon, which has had an auspicious beginning, shows promise of continuing to be a powerful and fruitful tool for future experiments. The use of very large dc magnetic fields of the order of 100 000 to 300 000 gauss together with long infrared and millimeter wavelengths combined with low-temperature techniques should make it possible to carry on resonance measurements on compound semiconductors, metals, and possibly alloys which have not yet yielded quantitative information by other techniques, except perhaps by the Azbel-Kaner effect. The galvanomagnetic and de Haas-van Alphen measurements are still very useful and should be pursued to provide information complementary to that obtained from the more modern methods of the cyclotron resonance and infrared magnetoabsorption experiments. The study of oscillatory magnetoabsorption is in its infancy, nevertheless, its possibilities for investigating a great many semiconductors looks bright. In addition to the anisotropy phenomenon, low-temperature measurements should yield information on fine structure leading to closer agreement between the quantum theory of magnetic levels of low quantum number than that provided by cyclotron resonance. The present experiments involve the interband transitions between magnetic levels in which the momentum is conserved. In the three materials studied so far, this has provided information about the energy bands at or near the center of the Brillouin zone. Another similar experiment can be carried out in the presence of a magnetic

[137] C. S. Smith, Phys. Rev. 94, 42 (1954).

field in which transitions are made between the impurity level and corresponding magnetic levels of the conduction or valence bands. Although the momentum is still conserved, one could study band extrema that are located anywhere in the Brillouin zone. For many of the semiconductors, these latter experiments will require low-temperature measurements at either liquid air or liquid helium. The possibility of improving and extending the usefulness of the oscillatory magneto-absorption effects will be greatly enhanced by the use of large dc magnetic fields of the order of 100 000 gauss or more.

ACKNOWLEDGMENTS

I would like to express my great appreciation to Mr. K. J. Button for editing, revising, and assembling this manuscript. His unusual editorial talent combined with his experience as an active physicist in this field has made it possible to transform a first draft into a final manuscript in a remarkably short period. I also want to thank Dr. J. G. Mavroides for reviewing the final manuscript, and I would like to acknowledge my indebtedness to Dr. S. Zwerdling, Dr. H. J. Zeiger, Dr. L. M. Roth, and Dr. J. G. Mavroides for discussions of their recent work in the various areas covered by this review.

Note added in proof.—Since the time this article was written, a number of new developments have been reported in the literature which should be briefly mentioned. In discussing the methods for studying the band structure of metals the important technique of the anomalous skin effect at zero magnetic field which has been reviewed by Pippard[138] and more recently by Chambers[139] should be included. Fawcett[140] has analyzed the anomalous skin resistance of tin for different orientations of the crystal to the surface in terms of ellipsoidal energy surfaces. Pippard[141] has carried out an analogous experiment for copper in order to determine the nature of the Fermi surface. Another scheme for studying the Fermi surface in metals, based upon the magnetoacoustic resonance observed by Bömmel[142] on tin at 4°K, was proposed by Pippard.[143]

The Azbel-Kaner resonance observed by Kip and co-workers[37] in tin with subharmonics up to fifteen in number confirm the initial findings of Fawcett.[35] The theoretical results of Azbel and Kaner have been derived by Heine[144] by using the ineffectiveness concept of Pippard including the magnetic field. Additional theoretical work of the original authors has been reported in greater detail[145] and includes a discussion of the experimental results of Fawcett and Aubrey and Chambers. Another point that requires clarification is that although the cyclotron resonance and the anomalous skin conditions are unfavorable with circularly polarized light, i.e., when the magnetic field is perpendicular to the sample, as shown by Chambers[146] and also Azbel and Kaganov,[147] this configuration is quite successful near the classical limit as in bismuth and graphite. This has again been clearly demonstrated by Datars and Dexter.[148] Their results on antimony for electrons agree with the values of Table I and they report that the energy surfaces for holes are ellipsoids of revolution with mass values $m_1=m_2=0.021m_0$ and $m_3=0.032m_0$. A detailed theoretical analysis of cyclotron resonance in graphite[32] has been given by Nozières.[149] In semiconductors, progress on cyclotron resonance has been made at infrared and millimeter wavelengths. Boyle and Brailsford[150] have reported resonance between bound Landau levels in InSb at 4°K from 70 to 120 μ and have found an electron mass $m^*=0.0146m_0$. Bagguley, Powell, and Taylor[151] have observed cyclotron resonance in gold-doped germanium at 77°K at 8.8 mm. Heller and co-workers[152] at Lincoln Laboratory have observed resonance in pure n-type germanium at 77°K and 2.65 mm.

The application of Onsager's results[153] to the theory of the de Haas-van Alphen effect by Lifshitz and Kosevich[154] and by Lifshitz and Pogorelov[155] has further strengthened its pre-eminent position as a tool for analyzing complicated Fermi surfaces in metals. One of the significant results is the generalization of the expressions in Eqs. (12) and (13) where $2\pi m^*\epsilon_0$ is replaced by $\mathcal{A}$, the area in momentum space of the orbit of the electron on the Fermi surface perpendicular to the magnetic field. Hence, as in cyclotron resonance, the effective mass is defined by $m^*=(d\mathcal{A}/d\epsilon_0)/2\pi$. These and other recent developments of the de Haas-van Alphen effect have been fully reviewed by Shoenberg[156] and Chambers.[139] The theory has been effectively applied to the experiments of Gunnersen[157] in evolving cushion-shaped Fermi surfaces for aluminum. Similarly, more involved energy surfaces were obtained

[138] A. B. Pippard, Advances in Electronics and Electron Phys. **6**, 1 (1954).
[139] R. G. Chambers, Can. J. Phys. **34**, 1395 (1956).
[140] E. Fawcett, Proc. Roy. Soc. (London) **A232**, 519 (1955).
[141] A. B. Pippard (to be published).
[142] H. E. Bömmel, Phys. Rev. **100**, 758 (1955).
[143] A. B. Pippard, Phil. Mag. **2**, 1147 (1957).
[144] V. Heine, Phys. Rev. **107**, 431 (1957).
[145] M. IA. Azbel and E. A. Kaner, Zhur. Eksptl. i. Teoret. Fiz. **32**, 896 (1957); M. IA. Azbel and E. A. Kaner, J. Phys. Chem. Solids, (to be published).
[146] R. G. Chambers, Phil. Mag. **1**, 459 (1956).
[147] M. IA. Azbel and M. I. Kaganov, Doklady Akad. Nauk. SSSR **95**, 41 (1954).
[148] W. R. Datars and R. N. Dexter, Bull. Am. Phys. Soc. Ser. II, **2**, 345 (1957).
[149] P. Nozières (to be published).
[150] W. S. Boyle and A. D. Brailsford, Phys. Rev. **107**, 903 (1957).
[151] Bagguley, Powell, and Taylor, Proc. Phys. Soc. (London) **A70** (1957).
[152] Stickler, Thaxter, Heller, and Lax (to be published).
[153] L. Onsager, Phil. Mag. **43**, 1006 (1952).
[154] I. M. Lifshitz and A. M. Kosevich, Doklady Akad. Nauk. SSSR **96**, 963 (1954); Zhur. Ekspl. i. Teoret. Fiz. **29**, 730 (1955).
[155] I. M. Lifshitz and A. V. Pogorelov, Doklady Akad. Nauk. SSSR **96**, 1143 (1954).
[156] D. Shoenberg, Progr. Low Temperature Phys. **II**, 227 (1957).
[157] E. M. Gunnersen, Phil. Trans. Roy. Soc. London **A249**, 299 (1957).

by Gold[158] from his de Haas-van Alphen data on lead.

Recent contributions on galvanomagnetic studies of energy bands in germanium and silicon have been reviewed by Glicksman.[159] The measurements of Long[160] on relatively pure silicon have been compared with theoretical results.[69] The work of Furth and Waniek[161] on magnetoresistance in germanium at 450 000 gauss has extended such measurements close to the saturation limit. Other semiconductors of interest investigated have been p-type lead telluride by Shogenji and Uchiyama[162] who find their results consistent with an ellipsoidal model with extrema along the [111] axes, and diamond where anisotropy data on p-type material by Mitchell and Wedepohl[163] suggested degenerate valence bands similar to that of germanium and silicon. The experimental work on metals has not been so extensive. However, the observation of the oscillatory effect of magnetoresistance in thin sodium wires by Babiskin and Seibenmann[164] has important implications for extending the usefulness of galvanomagnetic experiments in metals. The variation of the period with magnetic field is in accordance with the theoretical prediction of Sondheimer[165] for the magnetoresistance due to surface scattering in thin films.

Infrared absorption experiments by Macfarlane and co-workers[166] have detected fine structure in the absorption edge spectrum of germanium. The interpretation of these results in terms of indirect transitions with two phonons has reconciled the data with the position of the conduction band minima at the [111] edge of the Brillouin zone. The observation of fine structure of the oscillatory magnetoabsorption effect in germanium and the interpretation of the data by the Lincoln group[167] demonstrated the value of this technique in obtaining information about both the conduction and valence bands individually. It is now apparent that a similar phenomenon has been observed by Gross and co-workers[168] in cuprous oxide at low temperatures in the optical region at 29 000 gauss. Their observation of the Zeeman effect[169] of excitons in this material suggests another tool for studying the band structure of semiconductors. Exciton absorption of the direct transition was also definitely established by Zwerdling, Roth, and Lax[170] in germanium at 77°, 4°, and 1.5°K. The existence of such excitons has been considered theoretically by Dresselhaus and Elliot.[171] The magnetoabsorption measurements of these excitons up to 39 kilogauss were correlated with the theory of Yafet, Keyes, and Adams.[172] These new experiments indicate that anisotropy measurements of the Zeeman effect of excitons, as well as that of impurity levels of semiconductors, at low temperatures can provide quantitative information on the energy bands of semiconductors.

[158] A. V. Gold, Low Temperature Conference, Wisconsin, (August, 1957).
[159] M. Glicksman, Progr. Semiconductors 3, 1 (1958).
[160] D. Long, Phys. Rev. **107**, 672 (1957).
[161] H. P. Furth and R. W. Waniek, Phys. Rev. **104**, 343 (1956).
[162] K. Shogenji and S. Uchiyama, J. Phys. Soc. Japan **12**, 1164 (1957).
[163] E. W. J. Mitchell and P. T. Wedepohl, Proc. Phys. Soc. (London) **B70**, 527 (1957).
[164] J. Babiskin and P. G. Seibenmann, Phys. Rev. **107**, 1249 (1957).
[165] E. Sondheimer, Nature **164**, 920 (1949); Phys. Rev. **80**, 401 (1950).
[166] Macfarlane, McLean, Quarrington, and Roberts (to be published).
[167] Zwerdling, Lax, and Roth, Bull. Am. Phys. Soc. Ser. II, **3**, 16 (1958).
[168] Gross, Zakharchenia, and Pavinskii, Zhur. Tekh. Fiz. **27**, 2177 (1957).
[169] E. F. Gross and B. P. Zakhartchenia, J. Phys. radium **1**, 68 (1957).
[170] Zwerdling, Roth, and Lax (to be published).
[171] G. Dresselhaus, J. Phys. Chem. Solids **1**, 14 (1956); R. I. Elliot (to be published).
[172] Yafet, Keyes, and Adams, J. Phys. Chem. Solids **1**, 137 (1956).

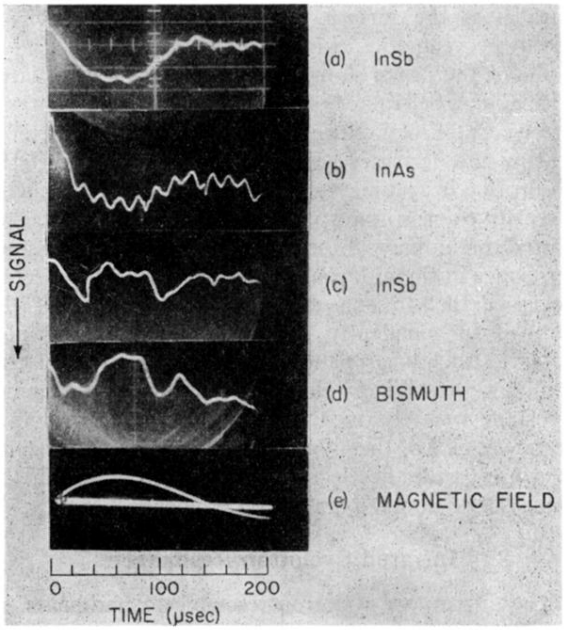

FIG. 13. Cyclotron resonance traces. Transmission signal through 200 μ samples at $\lambda = 12.7\,\mu$: (a) InSb, $B_{max} = 220$ kilogauss; (b) InAs, $B_{max} = 155$ kilogauss; (c) InSb, (d) bismuth. Magnetic field trace *vs* time shown by curve (e). (After Keyes, Zwerdling, Foner, Kolm, and Lax.)